## Reconstructing the Universe

J.Ambj m<sup>a;c</sup>, J.Jurkiew icz<sup>b</sup> and R.Loll<sup>c</sup>

<sup>a</sup> The Niels Bohr Institute, Copenhagen University Blegdam svej 17, DK-2100 Copenhagen , Denmark. em ail: ambjorn@nbidk

b M ark K ac C om plex System s R esearch C entre,
M arian Sm oluchow ski Institute of Physics, Jagellonian U niversity,
R eym onta 4, PL 30-059 K rakow, Poland.
em ail: jurkiew icz@ th.ifu jedu pl

<sup>c</sup> Institute for TheoreticalPhysics, Utrecht University, Leuvenlaan 4, NL-3584 CE Utrecht, The Netherlands. em ail: jambjorn@phys.uu.nl, r.loll@phys.uu.nl

#### A bstract

We provide detailed evidence for the claim that nonperturbative quantum gravity, de ned through state sums of causal triangulated geometries, possesses a large-scale limit in which the dimension of spacetime is four and the dynamics of the volume of the universe behaves semiclassically. This is a rest step in reconstructing the universe from a dynamical principle at the Planck scale, and at the same time provides a nontrivial consistency check of the method of causal dynamical triangulations. A closer look at the quantum geometry reveals a number of highly nonclassical aspects, including a dynamical reduction of spacetime to two dimensions on short scales and a fractal structure of slices of constant time.

### 1 Introduction

Nonperturbative quantum gravity can be de ned as the quest for uncovering the true dynamical degrees of freedom of spacetime geometry at the very shortest scales. Because of the enormous quantum—uctuations predicted by the uncertainty relations, geometry near the Planck scale will be extremely rugged and nonclassical. Although dierent approaches to quantizing gravity do not agree on the precise nature of these fundamental excitations, or on how they can be determined, most of the popular formulations agree that they are neither the smooth metrics g—(x) (or equivalent classical eld variables) of general relativity nor straightforward quantum analogues thereof. In such scenarios, one expects the metric to re-emerge as an appropriate description of spacetime geometry only at larger scales.

Giving up the spacetime metric at the Planck scale does not mean discarding geometry altogether, since geometric properties such as the presence of a distance function pertain to much more general structures than dierential manifolds with smooth metric assignments. One could hope that quantum gravity, when formulated in terms of the conjectured new microscopic degrees of freedom, was better behaved in the ultraviolet regime than standard perturbative approaches based on the spacetime metric. At the same time, it becomes a nontrivial test for such nonperturbative theories of quantum gravity whether they can reproduce the correct classical limit at su ciently large scales. However, using this as a consistency check to discriminate between good and bad candidate theories is in practice complicated by the fact that some explicit results about the quantum dynamics of the proposed quantum gravity theory must be known. For example, this is not yet the case in loop quantum gravity [2, 3, 4] or in four-dimensional spin foam models for gravity [5].

In the method of Causal Dynamical Triangulations one tries to construct a theory of quantum gravity as a suitable continuum limit of a superposition of spacetime geometries [6, 7, 8]. In close analogy with Feynman's famous path integral for the nonrelativistic particle, one works with an intermediate regularization in which the geometries are piecewise at<sup>2</sup>. The primary object of interest in this approach is the propagator between two boundary con gurations (in the form of an initial and nal spatial geometry), which contains the complete dynamical information about the quantum theory. Because of the calculational complexity

<sup>&</sup>lt;sup>1</sup>An exception are renormalization group approaches which look for nontrivial ultraviolet xed points in a metric formulation 1].

<sup>&</sup>lt;sup>2</sup>These are the analogues of the piecew ise straight paths of Feynman's approach. How-ever, note that the geometric congurations of the quantum-gravitational path integral are not imbedded into a higher-dimensional space, and therefore their geometric properties such as piecew ise atness are intrinsic, unlike in the case of the particle paths.

of the fill, nonperturbative sum over geom etries (the \path integral"), an analytical evaluation is at this stage out of reach. Nevertheless, powerful computational tools, developed in Euclidean quantum gravity [9, 10, 11, 12, 13, 14, 15] and other theories of random geometry (see [16] for a review), can be brought to bear on the problem.

This paper describes in detail how Monte Carlo simulations have been used to extract inform ation about the quantum theory, and in particular, the geom etry of the quantum ground state<sup>3</sup> dynam ically generated by superposing causal triangulations. It follows the announcement of several key results in this approach to quantum gravity, rst, a \quantum derivation" of the fact that spacetime is macroscopically four-dimensional [17], second, a demonstration that the large-scale dynamics of the spatial volume of the universe (the so-called \scale factor") observed in causal dynamical triangulations can be described by an effective action closely related to standard quantum cosmology [18], and third, the discovery that in the lim it of short distances, spacetime becomes e ectively two-dimensional, indicating the presence of a dynamically generated ultraviolet cuto [19]. They do not provide conclusive proof that our construction from st principles does lead to a viable theory of quantum gravity, but go som e way in establishing the existence of a physically meaningful classical limit. In addition, our detailed geom etric analysis throws some light on the highly nonclassical microscopic properties of the spacetimes dominating the gravitational path integral, which after all are higher-dimensional analogues of the nowhere-dimensional paths that provide the support of Feynm an's path integral.

Our presentation will proceed as follows. After recollecting some basic properties of the geom etric set-up of the regularized path integral over causal triangulations in Sec. 2, we explain in Sec. 3 how the path integral is implemented num erically. The statistical model underlying our construction possesses three phases, which are distinguished by the geometric nature of their ground states, as described in Sec. 4. From this point on, we concentrate on the phase which yields a ground state which is extended in time and space. In Sec. 5 we provide the detailed numerical evidence for why this state is four-dimensional at large scales and why its shape can be described by a minisuperspace action. We then em bark on a detailed investigation of substructures of the spacetime universe, namely, spatial slices (of xed integer time) in Sec. 6 and in Sec. 7 \thick spatial slices", which are geometries of nite time extension = 1. We measure both their Hausdor and spectral dimensions, the latter from a discrete diusion process. Interestingly, the geometry of the \thin" spatial slices shares some characteristics with a class of branched polymers which has already appeared in

<sup>&</sup>lt;sup>3</sup>Here and in the following, by \ground state" we will always mean the state selected by M onte Carlo simulations, performed under the constraint that the volume of spacetime is (approximately) kept—xed, a constraint we have to impose for simulation-technical reasons.

areas as diverse as noncritical string theory, econophysics and network theory. A sum mary of our results and an outlook are presented in Sec. 8.

### 2 Geometric set-up and simplicial action

We brie y rem ind the reader of the structure of the spacetime geometries which contribute to the regularized path integral [8]. The fundamental building blocks are two types of four-simplices \cut out of four-dimensional at Minkowski space. A at four-simplex of type (4,1) has six space-like edges of length-squared  $l_{\rm space}^2 = a^2$  and four time-like edges of length-squared  $l_{\rm ime}^2 = a^2$ . Similarly, a at four-simplex of type (3,2) has four space-like edges of length-squared  $l_{\rm space}^2 = a^2$  and six time-like ones of length-squared  $l_{\rm time}^2 = a^2$ . Each spacetime has a well-dened global foliation by a \proper time for time for 1 fig. 1 illustrates how the simplicial building blocks are situated between consecutive spatial slices of constant integer. The (4,1)-simplex consists of a spatial tetrahedron at time whose four vertices are connected by four time-like edges to the single vertex at time + 1. Similarly, the (3,2)-simplex consists of a spatial triangle at time whose vertices are connected to the two vertices at + 1 which form the end points of the fourth spatial edge of the simplex.

The way in which these building blocks, together with their counterparts with inversed time orientation, can form a spacetime slice of height =1 is by gluing them pairwise along a shared time-like boundary tetrahedron. In order to get a spacetime of time duration = t, one glues together t such slices in succession, which is of course only possible whenever their spatial boundary geometries at integer— match pairwise. We require the gluings to be such that the resulting discretized spacetime is a simplicial manifold. The spacetime topology is xed to [0;1]  $^{(3)}$ , where for our investigations we have chosen as constant— surfaces the three-spheres  $^{(3)}$  = S  $^3$ . For convenience in the computer simulations, we also sometimes identify time periodically, leading to a spacetime topology S  $^1$  S  $^3$ .

From the edge length assignments one can compute volumes and interior angles of the simplices which are needed because they appear in the Regge form of the Einstein action, from which the weight of each triangulated spacetime T in the sum over geometries will be computed (see [8] for calculational details). The gravitational action becomes then a simple function of a number of positive integers, which count the overall numbers of simplices or subsimplices of a certain type. For completeness, we give the explicit form of the action after analytic

<sup>&</sup>lt;sup>4</sup>W e choose the name \proper time" because the a priori integer-valued variable—can be extended continuously to the entire spacetime [20]. W ithin each simplex one can choose a coordinate system whose time variable coincides with—and also with the proper time of a freely falling observer in the simplex. Note that our setting here is that of piecew ise—at and not of smooth geometries.

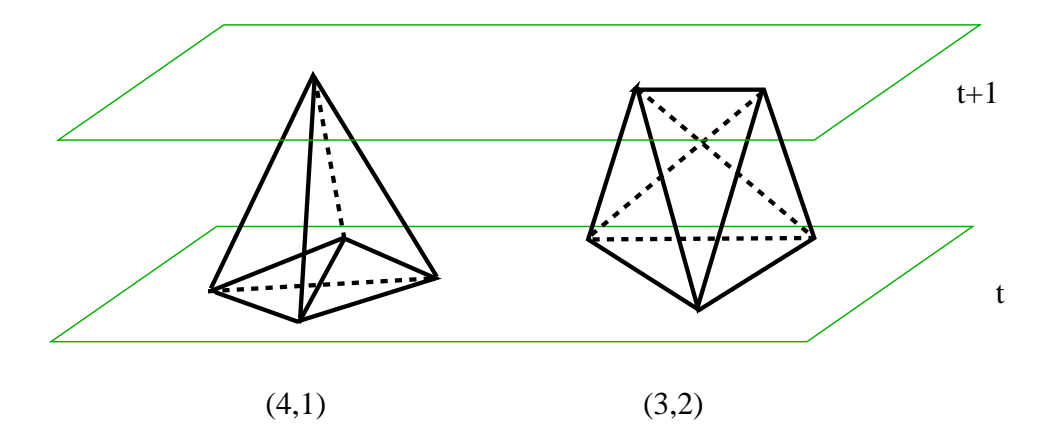


Figure 1: The two fundamental building blocks of causal dynamically triangulated gravity. The at four-simplex of type (4,1) on the left has four of its vertices at time and one at time + 1, and analogously for the (3,2)-simplex on the right. The \gap" between two consecutive spatial slices of constant integer time is led by copies of these simplicial building blocks and their time-reversed counterparts, the (1,4)- and the (2,3)-simplices.

continuation to the Euclidean sector, as a function of the number N  $_0$  of vertices (zero-sim plices), and the numbers N  $_4^{(3;2)}$  and N  $_4^{(4;1)}$  of four-sim plices of types (3,2) and (4,1) of either time orientation,

$$S_{E} = k^{(b)} \stackrel{p}{4} - 1 (N_{0})$$

$$+ N_{4}^{(4;1)} k^{(b)} \stackrel{p}{4} - 1 - \frac{p}{3} \arcsin \frac{p}{4} - \frac{1}{3} - \frac{p}{3} - \frac{1}{3} - \frac{1}{3}$$

In this expression, is the Euler characteristic of the piecew ise at four-manifold and  $\sim$  denotes the positive ratio between the two types of squared edge lengths after the Euclideanization. In order to satisfy the triangle inequalities, we need  $\sim > 7$ =12 [8]. For simplicity, we have assumed that the manifold is compact without boundaries. In the presence of boundaries, appropriate boundary terms must be added to the action.

For the simulations, a convenient alternative parametrization of the action is

given by

$$S_{E} = (_{0} + 6)N_{0} + _{4}(N_{4}^{(4;1)} + N_{4}^{(3;2)}) + (2N_{4}^{(4;1)} + N_{4}^{(3;2)});$$
(2)

where the functional dependence of the  $_{\rm i}$  and on the bare inverse Newton constant  $^{\rm (b)}$ , the bare cosm ological constant  $^{\rm (b)}$  and  $^{\rm (c)}$  and  $^{\rm (c)}$  and  $^{\rm (b)}$  are computed from (1). We have dropped the constant term proportional to  $^{\rm (b)}$ , because it will be irrelevant for the quantum dynam ics. Note that = 0 corresponds to  $\sim = 1$ , and is therefore a measure of the asymmetry between the lengths of the spatial and timelike edges of the simplicial geometry. As we shall see, the physically interesting region of the phase diagram of four-dimensional causal dynamical triangulations has positive  $^{\rm (b)}$ , which translates into values of  $^{\rm (c)}$  smaller than 1.

## 3 Numerical implementation

We have investigated the in nite-volume limit of the ensemble of causal triangulated four-dimensional geometries with the help of Monte Carlo simulations at nite four-volumes  $N_4 = N_4^{(4;1)} + N_4^{(3;2)}$  of up to 362.000 four-simplices. A simplicial geometry is stored in the computer as a set of lists, where the lists consist of dynamic sequences of labels for simplices of dimension n, 0 n 4, together with their position and orientation with respect to the time direction. Additional list data include information about nearest neighbours, i.e. how the triangulation hangs together, and other discrete data (for example, how many four-simplices meet at a given edge) which help improve the acceptance rate of Monte Carlo moves.

The simulation is set up to generate a random walk in the ensemble of causal geom etries of a xed time extension t. The local updating algorithm consists of a set of m oves that change the geom etry of the sim plicial m anifold locally, w ithout altering its topological properties. These can be understood as a Lorentzian variant of (a simpli ed version of) the so-called A lexander m oves [21, 22, 23], in the sense that they are compatible with the discrete time slicing of our causal geom etries. For example, the subdivision of a four-simplex into ve four-simplices by placing a new vertex at its centre is not allowed, because vertices can only be located at integer times  $\cdot$ . Details of the local moves can be found in  $\beta$ ]. A susual, each suggested local change of triangulation is accepted or rejected according to certain probabilities depending on the change in the action and the local geom etry. (Note that a move will always be rejected if the resulting triangulation violates the simplicial manifold property.) The moves are called in random order, with probabilities chosen in such a way as to ensure that the numbers of actually perform ed m oves of each type are approximately equal. We attained a rather high average acceptance rate of about 12.5%, which was made possible by keeping

track of sub-sim plex structures relevant for the perform ance of certain m oves, as mentioned earlier. The attempted m oves were performed in units of  $10^6$  (one \sweep"), with the time for one sweep approximately independent of the system volume in the region  $_0$  22 and 0.4:::0:6 where most of our measurements were taken.

In order to obtain an e cient sam pling of geom etries of large four-volum e (the larger the four-volum e, the better the com puter-generated geom etries describe the continuum lim it), we have perform ed the simulations at (approxim ately) constant four-volum e. This means that instead of the standard gravitational path integral (after Euclideanization)

$$Z_{E}(;G) = D[g]e^{S_{E}[g]}; S_{E}[g] = \frac{1}{G}^{Z} d^{4}x^{p} \frac{1}{\text{jdet}gj}(R 2)$$
 (3)

we simulate a discretized version of the path integral at xed four-volum e  $V_4$ ,

$$Z_{E}(V_{4};G) = D[g]e^{S_{E}[g]} \left( d^{4}x^{p} \overline{detg} V_{4}\right); \quad S_{E}[g] = \frac{1}{G}^{Z} d^{4}x^{p} \overline{detg}R;$$

$$(4)$$

which is related to (3) by a Laplace transform ation,

$$Z_{E}$$
 (;G) =  $\int_{0}^{Z_{1}} dV_{4} e^{\frac{1}{G} V_{4}} \widetilde{Z}_{E} (V_{4};G)$ : (5)

However, the localm oves do not in general preserve the numbers N  $_4^{(4;1)}$  and N  $_4^{(3;2)}$  of four-simplices, or indeed their sum. We deal with this in a standard way which was developed for dynamically triangulated models in dimensions three and four [24, 9] to ensure that the system volume is peaked at a prescribed value, with a well-dened range of uctuations. A dapting it to the current situation of causal triangulations with nonvanishing asymmetry, we implement an approximate four-volume constraint by adding a term

$$S = y_4^{(4;1)} \qquad y_4 \dot{y} \tag{6}$$

to the Euclidean action, with typical values of lying in the range of 0.01 to 0.02, except during them alization where we set = 0.05. The reason for xing  $N_4^{(4;1)}$  instead of  $N_4 = N_4^{(4;1)} + N_4^{(3;2)}$  in eq. (6) is mere technical convenience. We have checked in the phase space region relevant to four-dimensional quantum gravity (phase C, see below) that for  $N_4^{(4;1)}$  xed according to (6), the number  $N_4^{(3;2)}$  of four-simplices of type (3,2) is likewise very sharply peaked, see Fig. 2. The \four-volumes N\_4 and the corresponding \true" discrete four-volumes  $N_4$  used in the simulations are listed in Table 1. In order to stabilize the total volume after them alization,  $A_4$  has to be ne-tuned to its pseudo-critical value (which

\four-volum e" $N_4 = N_4^{(4;1)}$		20			
actual four-volum e N $_4$ = N $_4^{(4;1)}$ + N $_4^{(3;2)}$	22.25	45.5	91	181	362

Table 1: Translation table between the two types of discrete four-volum e,  $N_4$  and  $N_4$ , at which the num erical simulations reported in this article were performed, in units of 1000 building blocks (phase C only).

depends weakly on the volume) with accuracy smaller than , in practice to about 0.2. The measurements reported in this paper were taken at  $N_4 = 10$ , 20, 40, 80 and 160k, and the runs were performed on individual PCs or a PC farm for the smaller systems and a cluster of work stations for the larger systems.

Before measurements can be performed, one needs a well thermalized conquration of a given volume. In order to double-check the quality of the thermalization, we used two dierent methods to produce starting con gurations for the measurement runs. In the rst method, we evolved from an initial minim al four-dimensional triangulation of prescribed topology and of a given time extension t, obtained by repeated gluing of a particular triangulated space-time slice of = 1 and topology [0;1]  $S^3$ , which consists of 30 four-simplices. The spatial in- and out-geom etries of the slice are m in im alsoheres S<sup>3</sup>, m ade of ve tetrahedra. The two types of spatial boundary conditions used are (i) periodic identication of the geometries at initial and nalinteger times, and (ii) free boundary conditions, where all vertices contained in the initial slice at time of are connected by time like edges to a single vertex at time of 1, and similarly for the vertices contained in the nal spatial slice. From this initial con quration, the geometry evolves to its target volume  $N_4$  as specified through S. During the evolution the volume-volume correlator (see eq. (7) below) changes from a very broad distribution to the stable narrow shape seen in Fig. 7. The number of sweeps to reach the thermalized con guration changes linearly with  $N_4$  and ranged from  $10^5$  to  $10^8$  sweeps for the largest volumes, the latter of which took several weeks on a work station.

In the second method, we started instead from a thermalized con guration of smaller volume, which we let evolve towards the target volume. In this case the nalvolume-volume distribution is reached from a narrower distribution, namely, that of the smaller volume. During thermalization, this width grows very slowly. The timing of the entire process is similar to that of the rst method.

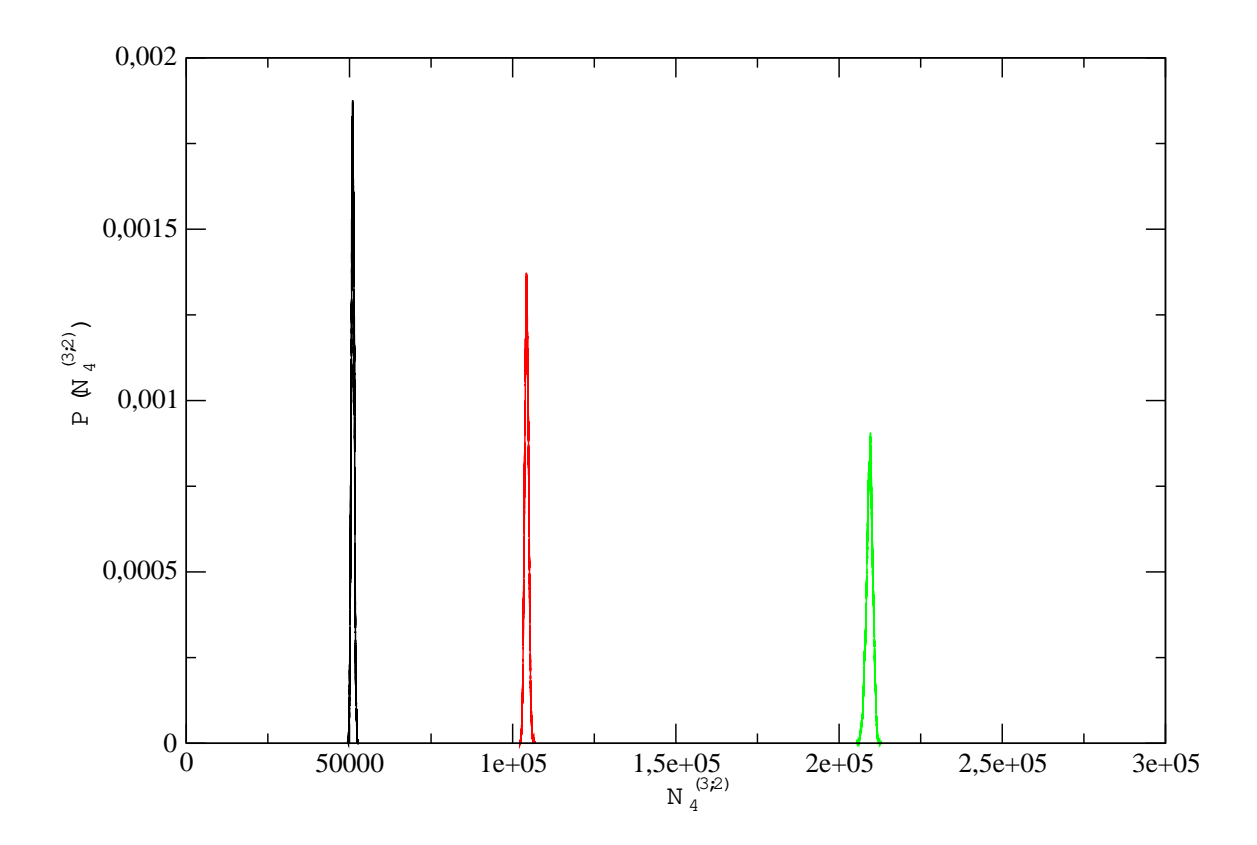


Figure 2: Unnormalized distribution of the number  $N_4^{(3;2)}$  of four-dimensional simplices of type (3,2), at xed numbers of four-simplices of type (4,1), for  $N_4^{(4;1)} = 40$ , 80 and 160k (left to right) at 0 = 2:2 and 0 = 0:6.

### 4 Phase structure of the model

Like always in dynam ically triangulated models, the bare cosmological constant  $^{(b)}$  (equivalently,  $_4)$  is tuned to its (pseudo-)critical value in the simulations, tantam ount to approaching the in nite-volume limit. Depending on the values of the two remaining parameters  $_0$  and in the discretized action (2), we have identified three different phases, A , B and C , mutually separated by lines of rst-order transitions. We have not yet measured their location in detail; Fig. 3 is a qualitative sketch of the phase diagram . We describe each of the three phases in tum:

(A) This phase prevails for su ciently large  $_0$  (recall  $_0$  is proportional to the bare inverse Newton's constant  $k^{(0)}$ ). When plotting the volume of the spatial slices = const as a function of , we observe an irregular sequence of maxima and minima, where the minimal size is of the order of the cuto,

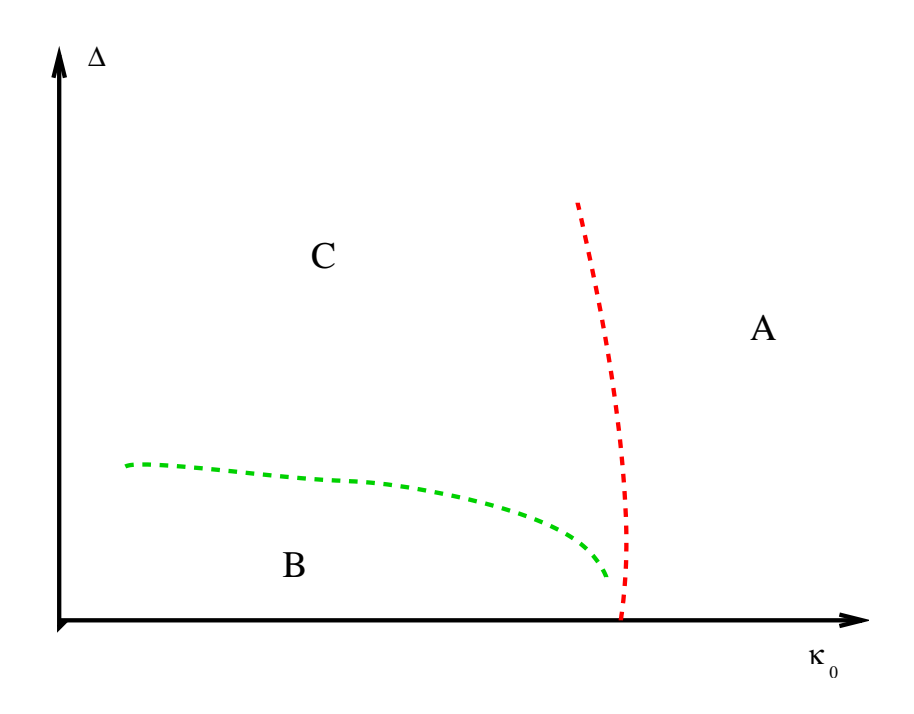


Figure 3: A qualitative sketch of the phase diagram of four-dim ensional causal dynam ical triangulations as function of the gravitational coupling  $_{\,\,0}$  and the asymmetry parameter .

and the sizes of the maxima vary, see Fig. 4. The time intervals during which the spacetime has a macroscopic spatial extension are small and of the order of = 3.

(B) This phase occurs for su ciently small  $_0$  and for small asymmetry , including = 0. In it, spacetime undergoes a \spontaneous dimensional reduction" in the sense that all four-simplices are concentrated in a slice of minimal time extension = 2, and the three-volume N  $_3$  () remains close to its kinematic minimum everywhere else (Fig. 5).

We believe that these two phases can be understood essentially from the dynam ics of the (Euclidean) geometries of the slices of constant—alone. The spatial slices in phase A are presumably realizations of branched polymers which dominate the path integral of three-dimensional Euclidean quantum gravity for large—0, whereas the extended part of the geometry in phase B corresponds to a Euclidean geometry in the so-called crumpled phase, which is characterized by the presence of very few vertices with extremely high coordination number [24, 42, 13, 14]. We will not elaborate here on our detailed measurements which quantify these statements, because we view phases A and B as lattice artifacts. However, there is yet another phase where the dynamics is not reduced to just the spatial directions

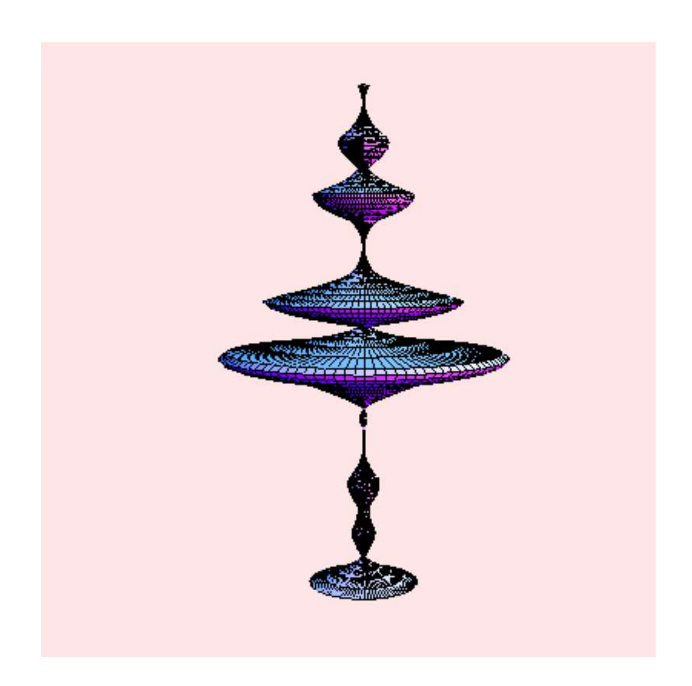


Figure 4: M onte C arlo snapshot of a typical universe in phase A ( $_0$  = 5:0, = 0), of discrete volume N  $_4$  = 45.5k and total time extent (vertical direction) t = 20. In this and the following two gures, the circum ference at integer proper time is chosen proportional to the spatial three-volume V  $_3$  (). The surface represents an interpolation between adjacent spatial volumes, without capturing the actual 4d connectivity between neighbouring spatial slices.

### but is genuinely four-dim ensional.

- (C) This phase occurs for su ciently small  $_0$  and nonvanishing asymmetry . In this phase, where >0 and  $\sim<1$  ( $\sim$  was de ned below eq. (1)), there seem s to be a su ciently strong coupling between successive spatial slices to induce a change in the spatial structure itself. We will discuss this new geometrical structure in detail in Sec. 6.
  - Of course, the presence of the asym metry parameter—is only possible because of the Lorentzian character of the model, and the resulting distinction between spatial and time directions. Since we implemented this distinction in the discretization by setting up a particular proper-time foliation and choosing arbitrary discrete length and time scales, it should not be surprising that in order to make contact with continuum physics, the ratio of these two scales cannot be chosen completely arbitrarily. This merely implies a restriction on the way the discretization is set up, and does not lead to any new parameters in the continuum theory. We have checked that the physical results derived within phase C do not depend on the numerical value of

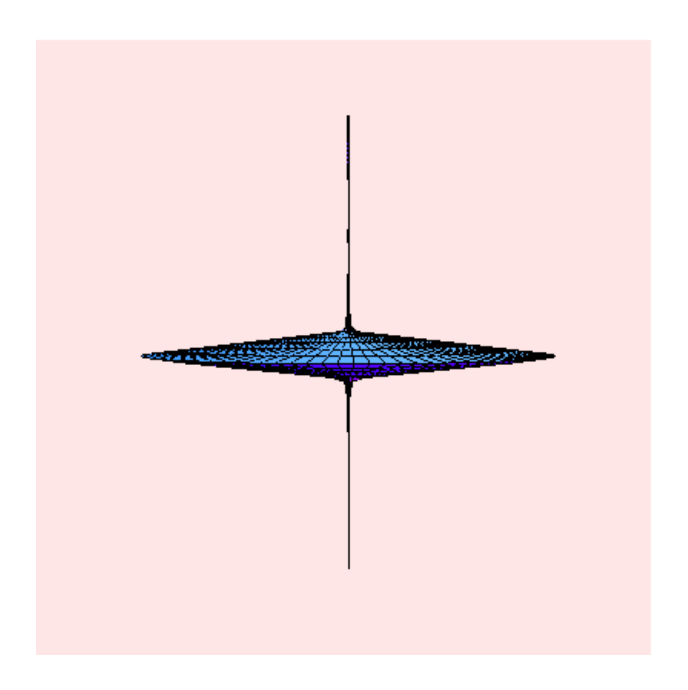


Figure 5: M onte Carlo snapshot of a typical universe in phase B ( $_0$  = 1:6), of discrete volum e N  $_4$  = 22.25k and total time extent t = 20. The entire universe has collapsed into a slice of m in in altime extension.

, within the allowed range. As we will see later, any such choice leads to the large-scale geometry of a homogeneous and isotropic universe.

The hallm ark of this phase is the presence of a stable extended four-geom etry, as rst reported in [17], and illustrated in Fig. 6. Not only does the macroscopic dimensionality of spacetime emerge with the correct classical value, but, equally remarkably, the global shape of the universe has been shown to be related to a simple minisuperspace action similar to those used in standard quantum cosmology [18]. Details of the computer measurements in this phase are the subject of Secs. 5-7 below.

Looking at the phase diagram of Fig. 3, it may at rst be surprising that one does not obtain a continuum lim it when the bare gravitational coupling constant (or New ton's constant) vanishes,  $G^{(b)}=1=k^{(b)}$ ! 0. However, one should bear in mind that the method of dynamical triangulation is a way of dening the path integral, rather than a regularization method which has nice smooth continuum manifolds as its dominant congurations as  $G^{(b)}$ ! 0.

A helpful analogy is the example of the (Euclidean) path integral for the relativistic particle, whose propagator G(x;y) can be represented as a sum over all random paths from x to y, whose action  $S(P) = m^{(b)}L(P)$  is given by the length L of the path P in target space, m ultiplied by a dimensionless bare m as parameter

m (b). If this path integral is regularized on a hypercubic lattice in R d, the possible paths are by de nition along the lattice links. Now consider R<sup>2</sup> and a path from (0;0) to the lattice point (x;y) = (an). No matter how small the lattice n;a spacing a and how large the number n of lattice steps, the lattice paths between the two points will never approach smooth continuum paths and their lengths will always be larger than  $\frac{1}{2} = \frac{1}{x^2 + y^2}$ . To de ne a continuum lim it for the lattice random walk one looks for critical points of the corresponding statistical system and studies the long-distance properties of suitable observables, in this case, of the propagator. The critical point is determined by the value of m (b), but this bare coupling constant is usually not related to the physical parameter (given here by the mass term in the continuum propagator) in a straightforward way (see [16, 25]) for details). In the case of dynam ical triangulations we follow a similar strategy. We do not a priori associate a continuum limit with certain values of the bare coupling constants. Rather, we look for points or regions in coupling-constant space where interesting scaling limits may exist. In the case of four-dim ensional gravity, it is natural to look for regions where some desirable features of m acroscopic spacetime are reproduced, and this is precisely the case for the phase-space region (C).

Let us also comment on how the continuum limit is taken in our approach. A coording to the standard, W ilsonian understanding of the relation between the theory of critical phenomena in statistical mechanics and quantumeld theory, in order to obtain a continuum quantum eld theory from an underlying regularized statistical system one needs to ne-tune a few coupling constants (corresponding to the relevant directions in coupling constant space) to reach the in nitedim ensional critical surface where a suitably de ned correlation length is in nite. D irections along the critical surface correspond to the in nitely many irrelevant (nonrenorm alizable) directions in coupling constant space. We inberg conjectured that this picture, which is usually believed to de ne ordinary renormalizable quantum eld theories, may generalize to quantum gravity, in the sense that it m ay have an associated, nonperturbatively de ned critical surface [26]. Several groups have since tried to substantiate this idea using either a (2+ )-expansion [27] or re ned renormalization group techniques [1]. Various lattice approaches to quantum gravity like quantum Regge calculus [28], Euclidean dynam ical triangulations [9, 29, 10] and the causal dynam ical triangulation of quantum gravity [17, 18, 8] used by us presently also endorse this picture.

In the latter, Lorentzian approach, the bare cosm ological constant must be netuned to obtain an in nite spacetime volume. Formally, we are not performing an analogous netuning of the bare gravitational coupling constant in phase C, which is nonstandard from a W ilsonian point of view. There are indeed lattice theories where no netuning is needed, and where an in nite-volume limit is su cient to identify a continuum limit, for example, the Coulomb phase of

U (1)-lattice gauge theory. However, the situation in gravity could be more involved, and subtleties may be buried in the identication of more complicated observables than the global ones we have considered so far. For a related discussion in three-dimensional causal dynamically triangulated quantum gravity, we refer to [30, 31]. What is important from our present point of view is the fact that the universes emerging from phase C satisfy the rst nontrivial tests of being viable candidates for quantum universes, as we will now turn to describe. Encouraged by these results, we are in the process of developing new and more re ned methods to probe the geometry of the model further, and which eventually should allow us to test aspects related to its local \transverse" degrees of freedom, the gravitons. We invite and challenge our readers to not such tests in a truly background-independent form alism of quantum gravity.

## 5 M easuring geom etry

Having generated a ground state of quantum geometry nonperturbatively, we would like to understand its geometric properties, in the sense of expectation values, which can be done in various ways. We will currently concentrate on the purely geometric observables, leaving the coupling to test particles and matter elds to a later investigation. We will proceed by rst determining a number of \rough properties of the quantum geometry such as its dimensionality and its global scaling properties. These properties of quantum spacetime play an important role, because for any viable candidate theory of quantum gravity, they must be shown to reproduce the correct classical limit at su ciently large scales, namely, geometry as described by Einstein's general theory of relativity.

As we have emphasized in [17], in nonperturbative models of quantum gravity, where by denition geometry uctuates very strongly at short scales, there is absolutely no guarantee that any sensible classical limit is obtained even for very basic quantities like the dimension of spacetime. Indeed, previous formulations which can probe the dimensionality of geometry numerically through the scaling behaviour of suitable observables, for example, dynamically triangulated models of Euclidean quantum gravity, have not come up with evidence for the value 4. Instead such models seem to run generically into highly degenerate geometries of one type or other [10, 32, 12, 14], which at large scales have nothing to do with four-dimensional spacetime as we know it. From this it seems likely that the condition of obtaining the correct classical limit imposes strong constraints on any attempt to quantize gravity nonperturbatively and background-independently. Of course, proposals of quantizing gravity are often not su ciently developed to decide whether they can reproduce classical geometry from rst principles, without putting in a preferred background structure along the way.

In the following, we will present a detailed discussion of a number of geometric properties of the extended ground state of phase C above. Several main results were already announced in our previous publications [17, 18, 19]. The picture emerging so far is that of a geometry whose large-scale properties are classical, but whose detailed microscopic structure is highly complicated and nonclassical. We will proceed by rst presenting the evidence for the macroscopic four-dimensionality of spacetime, and then describing the insights into the geometric structure obtained from measuring quantities associated with slices of constant time.

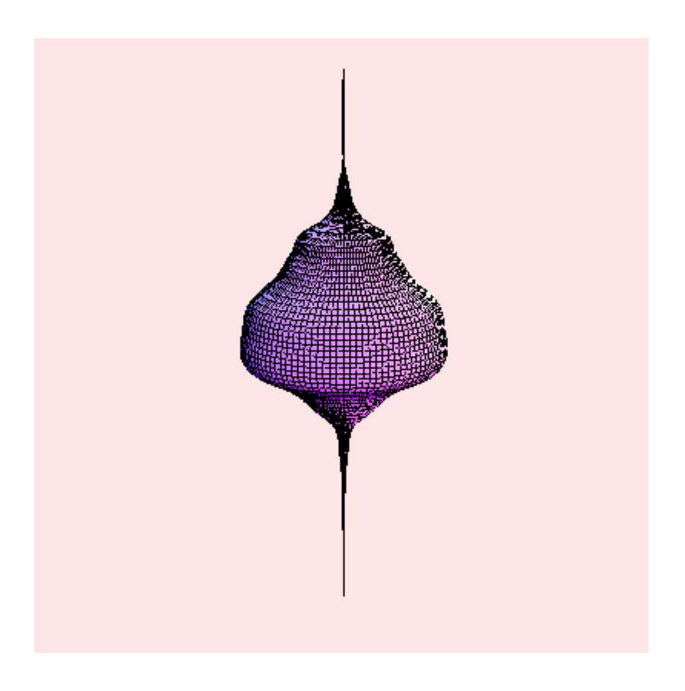


Figure 6: M onte Carlo snapshot of a typical universe in phase C ( $_0$  = 2:2) of discrete volum e N  $_4$  = 91.1k and total tim e extent t= 40.

# 5.1 The evidence for spacetime dimension four: Global scaling

As illustrated by Fig. 6, the total four-volume is distributed over the t time steps (we are working with a periodic identication in the time direction) in a characteristic way. At a given discrete four-volume, for su ciently large t the conguration separates out into a thin \stalk" whose four-volume at each time step uctuates little and is close to the kinematically allowed minimum for the topology [0;1] S³, and an extended, blob-shaped structure, the \universe". The average volumes per time step = 1 of the stalk is practically independent of the

total volume of the system, with s 25.5 for the range of coupling constants we used. As explained in Sec. 3, we measure the spacetime volume by  $N_4$ , that is, in units of four-simplices of type (4,1). Since every spatial tetrahedron is contained in exactly two (4,1)-simplices, the average three-volume  $N_3$  ( ) at integer time in the stalk is therefore given by s=2.

A suitable observable for studying the large-scale structure of the universe is the volum e-volum e correlator<sup>5</sup>

$$C_{N_4}()$$
  $h_3(0)N_3()i = X^t \frac{4h(N_3()) s=2)(N_3(+) s=2)i}{(N_4 ts)^2};$  (7)

which satis es the normalization condition

$$\overset{X^{1}}{C}_{N_{4}}() = 1;$$
(8)

where a periodic identi cation of the time variable has been assumed. Because of the subtraction of the cuto volume s=2, the volume-volume correlator is only sensitive to the extended part of the geometry, and measures the distribution of the \e ective" four-volume

$$N_4^e = N_4^e$$
 ts (9)

contained in it. We have measured the distribution (7) for system sizes  $N_4 = 10$ , 20, 40, 80 and 160k, at  $_0 = 2.2$ , = 0.6 and t= 80. We expect the distribution to scale as a function of  $N_4$ , with an underlying universal distribution

$$C_{N_4}(x) := (N_4^e)^{1=D_H} C_{N_4}((N_4^e)^{1=D_H} x)$$
 (10)

depending on the rescaled time variable<sup>6</sup>

$$X = \frac{1}{(N_4^e)^{1=D_H}} :$$
 (11)

The value of the scaling dimension D $_{\rm H}$  is then determined by the method of \best overlap". In it, we compare each measured distribution with that of the 40k system. In order to provide a comparison point for each value of x and to quantify the overlap, we set performed a spline interpolation of the discrete distribution at 40k. Fig. 7 shows a combined plot of the rescaled distributions, using D $_{\rm H}$  = 4 as a scaling dimension, and with a plot range symmetrized around x = 0. The overlap is nearly perfect. As can be read o Fig. 8, which shows the average error of the overlap as a function of D $_{\rm H}$ , the best overlap corresponds to D $_{\rm H}$  3.8 0.25. We take this outcome as strong evidence that our spacetimes

<sup>&</sup>lt;sup>5</sup>N ote that in the analogous relation (6) in [17] we m istakenly om itted the ensemble averages on the right-hand side.

 $<sup>^6</sup>$ W e are employing standard nite-size scaling methods familiar from the theory of critical phenomena (see [33] for a textbook exposition), adjusted to our problem.

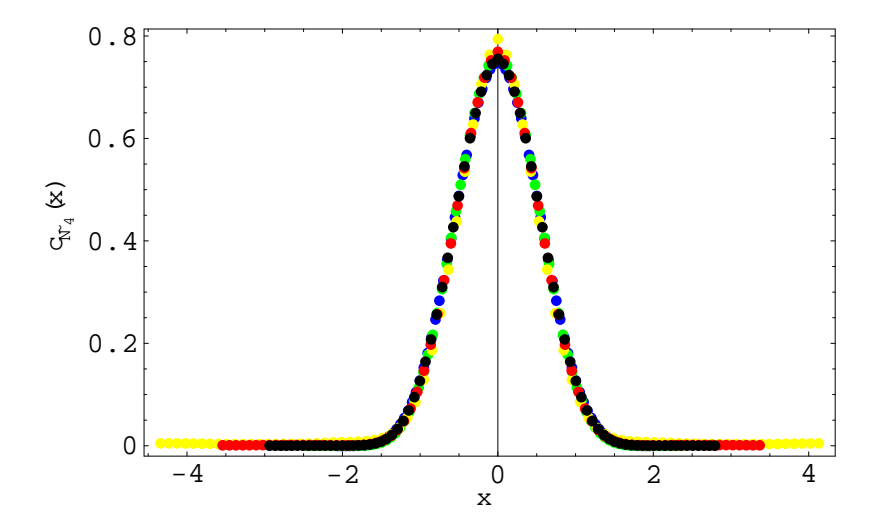


Figure 7: The scaling of the volum e-volum e distribution, as function of the rescaled time variable  $x = (N_4^e)^{1-4}$ . Data points come from system sizes  $N_4 = 10$ , 20, 40, 80 and 160k at  $_0 = 22$ ,  $_0 = 0.6$  and t= 80.

are genuinely four-dimensional at large scales.

## 5.2 The evidence for spacetime dimension four: Spectral dimension

A nother way of obtaining an elective dimension of the nonperturbative ground state, its so-called spectral dimension D  $_{\rm S}$ , is from studying a division process on the underlying geometric ensemble. On a d-dimensional manifold with a xed, smooth R iemannian metric  $g_{ab}$  (), the division equation has the form

$$\frac{Q}{Q} K_g(;_0;_0) = {}_{g}K_g(;_0;_0;_0);$$
 (12)

where is a ctitious di usion time,  $_g$  the Laplace operator of the metric  $g_{ab}$  ( ) and K  $_g$  ( ;  $_0$ ; ) the probability density of di usion from  $_0$  to  $_0$  in di usion time

<sup>&</sup>lt;sup>7</sup>Of course, we will never be able to show by computer simulations alone that the elective dimension is exactly equal to four. What we are assuming here is that this dimension is indeed an integer, because there are no classical theories describing the dynamics of geometries of dimensionality 3.9, say. Also, it is known from the measurement of Hausdor dimensions in two-dimensional Euclidean quantum gravity (where it can be proven that the Hausdor dimension is four (!) [34, 35]) that the computer simulations tend to slightly underestimate the actual values [36, 37].

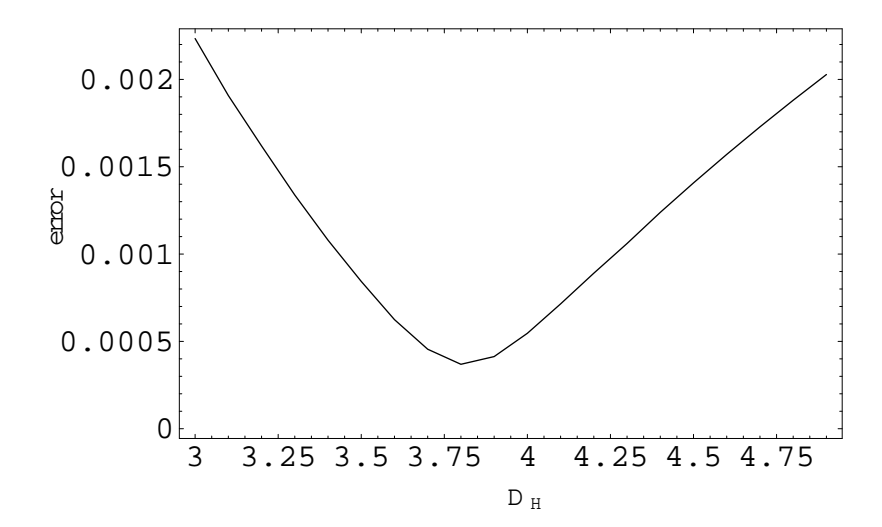


Figure 8: Estimating the best scaling dimension  $D_{\rm H}$  from optimal overlaps of rescaled volume-volume distributions. The plot variable is the average error of the overlap as function of  $D_{\rm H}$ .

. We will consider disusion processes which initially are peaked at some point  ${\color{black}0}$  ,

$$K_g(;_0;_0;_0) = \frac{1}{\det g(;_0)} d(;_0);$$
 (13)

For the special case of a at Euclidean metric, we have

$$K_g(;_0;_0;_0) = \frac{e^{d_g^2(;_0)=4}}{(4)^{d=2}}; \qquad g_{ab}() = {}_{ab}$$
: (14)

For general curved spaces K  $_{\rm q}$  has the well-known asym ptotic expansion

$$K_g(;_0;)$$
  $\frac{e^{d_g^2(;_0)=4}}{d=2} X^{i}$   $a_r(;_0)$  r (15)

for small , where  $d_g$  (; 0) denotes the geodesic distance between and 0. Note the appearance of the power del in this relation, rejecting the dimension dof the manifold, just like in the formula (14) for at space. This happens because small 's correspond to short distances and for any given smooth metric short distances in ply approximate atness.

A quantity that is easier to m easure in num erical simulations is the average return probability  $P_{\rm g}$  ( ), which possesses an analogous expansion for small ,

$$P_{g}()$$
  $\frac{1}{V}^{Z}$   $d^{d}$   $p$   $\frac{1}{\det g()} K_{g}(;;)$   $\frac{1}{d=2} X^{d} A_{r}^{r};$  (16)

where V is the spacetime volume  $V = \begin{bmatrix} R & p \\ d^d & detg() \end{bmatrix}$  and the expansion coecients  $A_r$  are given by

$$A_r = \frac{1}{V}^Z d^d P \frac{1}{\det g(\cdot)} a_r(\cdot; \cdot)$$
 (17)

For an in nite at space, we have  $P_g$  ( ) = 1=(4 ) $^{d=2}$  and thus can extract the dim ension d by taking the logarithm ic derivative,

$$2\frac{d \log P_g()}{d \log} = d; \tag{18}$$

independent of . For non at spaces and/or nite volume V, one can still use eq. (18) to extract the dimension, but there will be corrections for sulciently large . For nite volume in particular,  $P_g$  ( ) goes to 1=V for  $V^{2=d}$  since the zero mode of the Laplacian  $_g$  will dominate the dilusion in this region. For a given dilusion time the behaviour of  $P_g$  ( ) is determined by eigenvalues  $_n$  of  $_g$  with  $_n$  1= , and the contribution from higher eigenvalues is exponentially suppressed. Like in the at case, where dilusion over a time  $_g$  probes the geometry at a linear scale  $_g$ , large  $_g$  corresponds to large distances away from the origin  $_g$  of the dilusion process, and small to short distances.

The construction above can be illustrated by the simplest example of diusion in one dimension. The solution to the diusion equation on the real axis is

$$K (;) = \frac{e^{\frac{2-4}{4}}}{4}; \quad K (k;) = e^{k^2};$$
 (19)

where K (k; ) denotes the Fourier transform of K (; ). The eigenvalues of the Laplace operator are of course just given by  $k^2$ . In order to illustrate the nite-volume e ect, let us compactify the real line to a circle of length L. The return probability is now given by

$$P_{L}() = \frac{1}{L} \sum_{n=1}^{X^{L}} e^{k_{n}^{2}} = \frac{1}{4} \sum_{m=1}^{X^{L}} e^{L^{2}m^{2}=4}; \quad k_{n} = \frac{2n}{L};$$
 (20)

where in the second step we have performed a Poisson resummation to highlight the  $^{1=2}$ -dependence for small . In line with the discussion above, the associated spectral dimension D  $_{\rm S}$  ( ) is constant (and equal to one) up to -values of the order L  $^2=4$   $^2$ , and then goes to zero monotonically.

In applying this set-up to four-dimensional quantum gravity in a path integral formulation, we are interested in measuring the expectation value of the return probability  $P_g$  ( ). Since  $P_g$  ( ) de ned in (16) is invariant under reparametrizations, it makes sense to take its quantum average over all geometries of a given

spacetim e volum e V4,

$$P_{V_4}() = \frac{1}{Z_E(V_4)} Z_{D[g_{ab}]} e^{S_E(g_{ab})} (d^4x) \frac{Z}{\det g} V_4) P_g(); \qquad (21)$$

where the partition function  $\mathcal{Z}_E$  and the corresponding gravitational action  $\mathcal{S}_E$  were de ned in (4). Since the small-behaviour of  $P_g$  ( ) is the same for each smooth geometry, it might seem obvious that the same is true for their integral  $P_{V_4}$  ( ), but this need not be so. Firstly, the scale in (21) is held xed, independent of the geometry  $g_{ab}$ , while the expansion (16) contains reference to higher powers of the curvature of  $g_{ab}$ . Secondly, one should keep in mind that a typical geometry which contributes to the path integral { although continuous { is unlikely to be smooth. This does not invalidate our treatment, since diusion processes can be meaningfully de ned on much more general objects than smooth manifolds. For example, the return probability for diusion on fractal structures is well studied in statistical physics and takes the form

$$P_{N} () = {}^{D} {}_{S} = {}^{2} F \frac{1}{N^{2=D} {}_{S}} ;$$
 (22)

where N is the \volume" associated with the fractal structure and D $_{\rm S}$  the so-called spectral dimension, which is not necessarily an integer. An example of fractal structures are branched polymers (which will play a role in Sec. 6 below when we analyze the geometry of spatial slices), which generically have D $_{\rm S}=4=3$  [38, 39]. Extensive numerical simulations [40, 41] have shown that in 2d quantum gravity the only elect of integrating over geometries is to replace the asymptotic expansion (16), which contains reference to powers of the curvature related to a specilic metric, by the simpler form (22).

Our next task is to de ne di usion on the class of m etric spaces under consideration, the piecew ise linear structures de ned by the causal triangulations T. We start from an initial probability distribution

$$K_{T}(i;i_{0};=0)=_{i;i_{0}};$$
 (23)

which vanishes everywhere except at a random ly chosen (4,1)-sim plex  $i_0$ , and de ne the di usion process by the evolution rule

$$K_{T}(j;i_{0}; + 1) = \frac{1}{5} K_{T}(k;i_{0}; ):$$
 (24)

These equations are the simplicial analogues of (13) and (12), with the triangulation (together with its Euclideanized edge-length assignments) playing the role

of  $g_{ab}$ , and k! j denoting the ve nearest neighbours of the four-simplex j. In this process, the total probability

$$X K_{T}(j;i_{0};) = 1$$
 (25)

is conserved. The return probability to a sim plex  $i_0$  is then de ned as  $P_T$  ( $i_0$ ; ) =  $K_T$  ( $i_0$ ;  $i_0$ ; ) and the quantum average as

$$P_{N_{4}}() = \frac{1}{Z_{E}(N_{4})} \sum_{T_{N_{4}}}^{X} e^{S_{E}(T_{N_{4}})} \frac{1}{N_{4}} \sum_{i_{0} \geq T_{N_{4}}}^{X} K_{T_{N_{4}}}(i_{0}; i_{0}; ); \qquad (26)$$

where  $T_{N_4}$  denotes a triangulation with  $N_4$  four-simplices, and  $S_E$  ( $T_{N_4}$ ) and  $T_E$  ( $N_4$ ) are the obvious simplicial analogues of the continuum quantities (4) at xed four-volume. Assuming that the return probability behaves according to (22), with  $N=N_4$ , we can extract the value of the fractal dimension  $D_S$  by measuring the logarithm is derivative as in (18) above, as long as the diffusion time is not much larger than  $N_4^{2=D_S}$ ,

$$D_S() = 2 \frac{d \log P_{N_4}()}{d \log} + \text{ nite-size corrections:}$$
 (27)

From the experience with numerical simulations of 2d Euclidean quantum gravity in terms of dynamical triangulations [37, 40, 41], we expect some irreqularities in the behaviour of the return probability for the smallest , i.e. close to the cut-o scale. Typically, the behaviour of  $P_{\rm N}$  ( ) for odd and even disusion steps will be quite discret for small and merge only for 20 30. A fter the merger, the curve enters a long and stable regime where the right-hand side of (27) is independent of , before nite-size e ects start to dominate which force it to go to zero. (A lso the 3d Euclidean hypersurfaces of constant time in our current set-up show a very similar behaviour, as can be seen in Fig. 15.)

The origin of the odd-even asymmetry can again be illustrated by the simple case of di usion on a one-dimensional circle, whose solution is the discretized version of the solution (20). In this case the asymmetry of the return probability between odd and even time steps is extreme: if we use the two-dimensional version of the simple evolution equation (24), we obtain

as long as < L=2, where L is the discrete volume of the circle (i.e. the number of its edges). It is of course possible to eliminate this asymmetry by using an

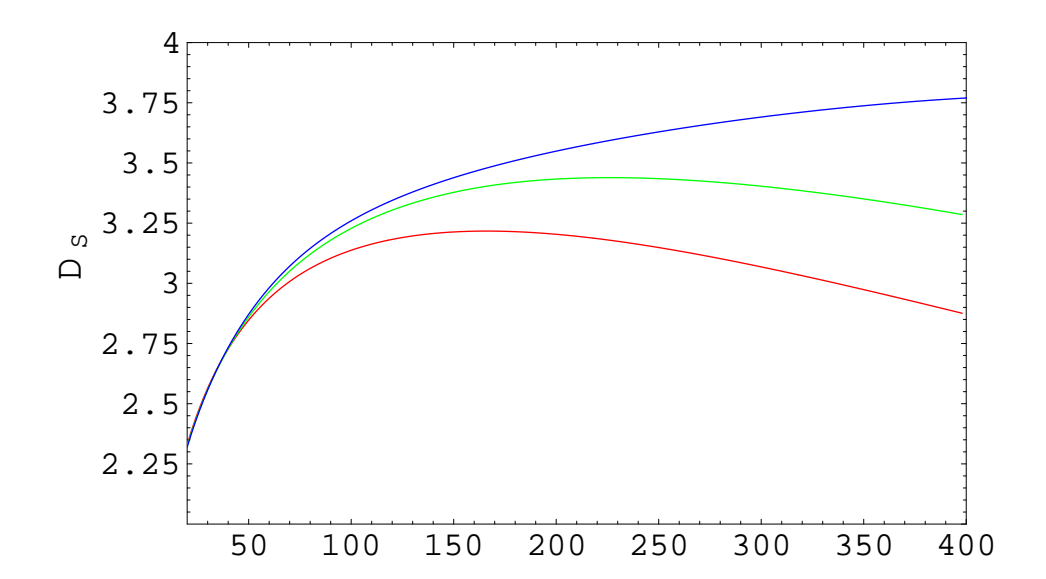


Figure 9: The spectral dim ension D  $_{\rm S}$  ( ) of causal dynam ical triangulations as a function of the di usion time , which is a direct measure of the distance scale probed. The measurements were taken at volumes N  $_4$  = 20k (bottom curve), 40k and 80k (top curve), and for  $_0$  = 2:2, = 0:6 and t= 80.

\improved" discretized di usion equation, but in the case of higher-dim ensional random geom etries like the ones used in 4d causal dynam ical triangulations this is not really necessary. The random connectivity will elim inate the asymmetry after a number of steps as exemplied by Fig. 15.

The results of measuring the spacetime spectral dimension D  $_{\rm S}$  were instituted in [19]. We work with system sizes of up to N  $_4$  = 80k with  $_0$  = 2.2, = 0.6 and t= 80. Since we are interested in the bulk properties of quantum spacetime and since the volume is not distributed evenly in the time direction (cf. Fig. 6), we always start the direction process from a four-simplex adjacent to the slice of maximal three-volume. When this is done the variations in the curve D  $_{\rm S}$  () for direct generic choices of T  $_{\rm N}$  and starting simplices i  $_0$  are small, as long as i  $_0$  is located not too close to the stalk. The data curves presented in Fig. 9 were obtained by averaging over 400 direct direct direction out to a time = 400 is rather time-consuming and the variation in P  $_{\rm T}$  (i  $_0$ ; ) as a function of T and i  $_0$  (with the initial conditions specified above) is small, we have not performed a more extensive average over configurations. We have omitted error bars from Fig. 9 to illustrate how the curves converge to a shape that represents D  $_{\rm S}$  () in

the in nite-volume limit, and which is given by the envelope of the data curves for nite volume. For the two lower volumes,  $N_4 = 20k$  and  $N_4 = 40k$ , there still are clear nite-volume exists across the extra clear nite-volume exists.

By contrast, the top curve { corresponding to the maximal volume  $N_4 = 80$ k { continues to rise for increasing , which makes it plausible that we can ignore any nite-size e ects and that it is a good representative of the in nite-volume limit in the -range considered. We will therefore concentrate on analysing the shape of this curve, which is presented separately in Fig. 10, now with error bars included. (More precisely, the two outer curves represent the envelopes to the tops and bottoms of the error bars.) The error grows linearly with , due to the occurrence of the log in (27).

The rem arkable feature of the curve D  $_{\rm S}$  ( ) is its slow approach to the asym ptotic value of D  $_{\rm S}$  ( ) for large . A sem phasized in [19], this type of behaviour has never been observed previously in systems of random geometry, and again underlines that causal dynamical triangulations in four dimensions behave qualitatively dierently, and that the quantum geometry produced is in general richer. The new phenomenon we observe here is a scale dependence of the spectral dimension, which has emerged dynamically. This is to be contrasted with fractal structures which show a self-similar behaviour at all scales, and which lead to D  $_{\rm S}$  ( )-curves like that shown in Fig. 15.

As explained in [19], the best three-parameter twhich asymptotically approaches a constant is of the form

$$D_{S}() = a \frac{b}{+c} = 4.02 \frac{119}{54+}$$
: (29)

The constants a, b and c have been determined by using the full data range 2 [40;400] and the curve shape agrees well with the measurements, as can be seen from Fig. 10. Integrating (29) we obtain

P ( ) 
$$\frac{1}{a=2(1+c=)^{b=2c}}$$
; (30)

from which we deduce the limiting cases

<sup>&</sup>lt;sup>8</sup> In both Figs. 9 and 10 we have only plotted the region where the curves for odd and even coincide, in order to exclude short-distance lattice artifacts. The two curves merge at about = 40. Since the di usion distance grows as \_\_\_, a return di usion time of 40 corresponds to just a few steps away from the initial four-simplex.

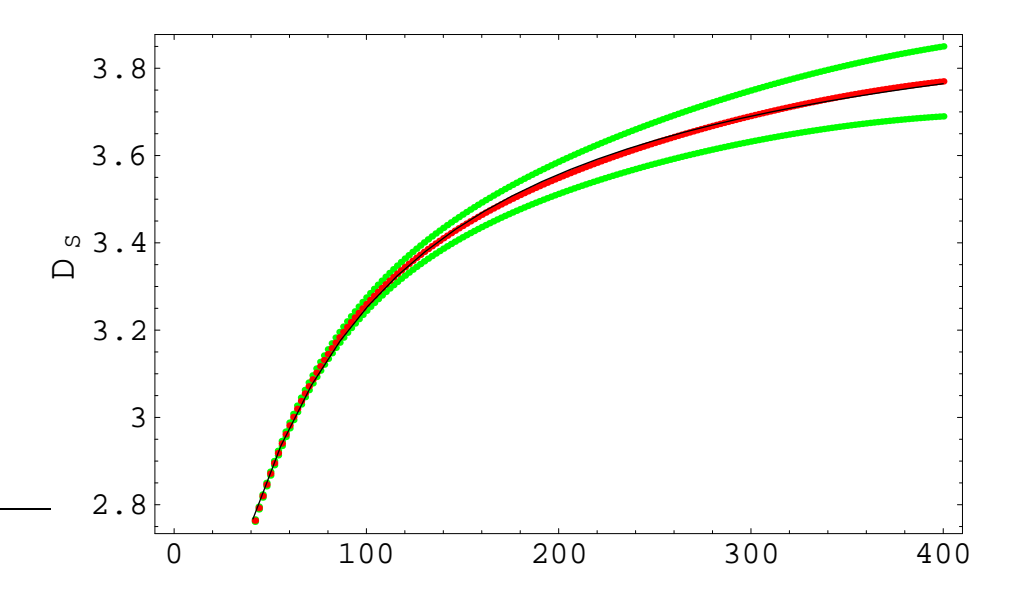


Figure 10: The spectral dim ension D  $_{\rm S}$  of the universe as function of the di usion time , measured for  $_0$  = 22, = 0:6 and t= 80, and a spacetime volume N  $_4$  = 181k. The averaged measurements lie along the central curve, together with a superimposed best tD  $_{\rm S}$  () = 4:02 119=(54+ ). The two outer curves represent error bars.

We conclude that the quantum geom etry generated by causaldynam ical triangulations has a scale-dependent spectral dimension which increases continuously from a b=c to a with increasing distance. Substituting the values for a, b and c obtained from the t (29), and taking into account their variation as we vary the range [ $_{m \text{ in}}$ ;  $_{m \text{ ax}}$ ] and use dierent weightings for the errors, we obtained the asymptotic values [19]

$$D_{S} (=1) = 4.02 0.1 (32)$$

for the \long-distance spectral dim ension" and

$$D_{S}(=0) = 1.80 \quad 0.25$$
 (33)

for the \short-distance spectral dimension". A dynam ically generated scale-dependent dimension with this behaviour is truly exciting news, because it signals the existence of an elective ultraviolet cut-o for theories of gravity with and without matter coupling, brought about by the (highly non-perturbative) behaviour of the quantum -geometric degrees of freedom on the very smallest scale.

### 5.3 The e ective action

In order to get a more detailed understanding of the geometric properties of our universe, we next attempt to reproduce the overall shape of the universe of Fig.

6 (in other words, the behaviour of its three-volum e  $V_3$  as a function of time) from an elective action for the single variable  $V_3$  ( ), valid at su ciently large scales  $V_3$  1. This will enable us to compare our results with those from so-called minisuperspace models. The simplest such models also take the form of dynamical systems of a single variable, namely, the scale factor a ( ), describing the linear spatial extension of the universe and related to the three-volume by

$$V_3() / a^3()$$
: (34)

D espite the resemblance, the status of our derivation is very dierent from that of a m inisuperspace model. In the latter, one works from the outset in a drastically truncated fram ework, where the classical dynam ics of the entire universe is described by the variable a() instead of the full metric data  $q_j$  (;x). For closed universes, and in (Euclidean) proper-time coordinates, this corresponds to considering line elements of the form

$$ds^2 = d^2 + a^2 () d_3^2;$$
 (35)

where d  $^2_3$  denotes the metric on the three-sphere. The corresponding Einstein-Hilbert action is

$$S^{m \text{ ini}} = \frac{1}{G} Z$$
 ! ! !  $\frac{da()}{d} a() + \mathring{a}();$  (36)

including a cosm ological constant. These m in isuperspace m odels are often taken as starting point for a path integral quantization, leading to quantum cosm ologies like those used by Hartle and Hawking in their sem iclassical evaluation of the wave function of the universe [43] (see also [44, 45, 46, 47, 48, 49, 50, 51] for related work). The hope is that such a truncated version of quantum gravity still describes some features of the full theory correctly.

By contrast, the central feature of dynam ical triangulations is a bona depath integration over all geometric degrees of freedom (which in particular will have a nontrivial spatial dependence), without appealing to any symmetry reduction, either classical or quantum -mechanical. In the nal result, one may then decide to keep track only of the three-volume (equivalently, the scale factor) as a dynamical variable and try to extract its elective large-scale behaviour. It is an interesting question whether the two approaches (that is, truncating the degrees of freedom before or after the quantization) are equivalent. In view of the severe diculties in making quantum-cosmological path integrals well-de ned and convergent [49], one might hope that they are not. This is indeed the conclusion from the ndings

 $<sup>^{9}</sup>$ W e work with Euclidean signature in order to facilitate comparison with the simulation data, which also describe Euclidean, W ick-rotated geometries.

in causal dynam ical triangulations we are about to describe. As we will see, the collective e ect of the full quantum -gravitational degrees of freedom changes the dynam ical description in terms of the single scale factor in a drastic way.

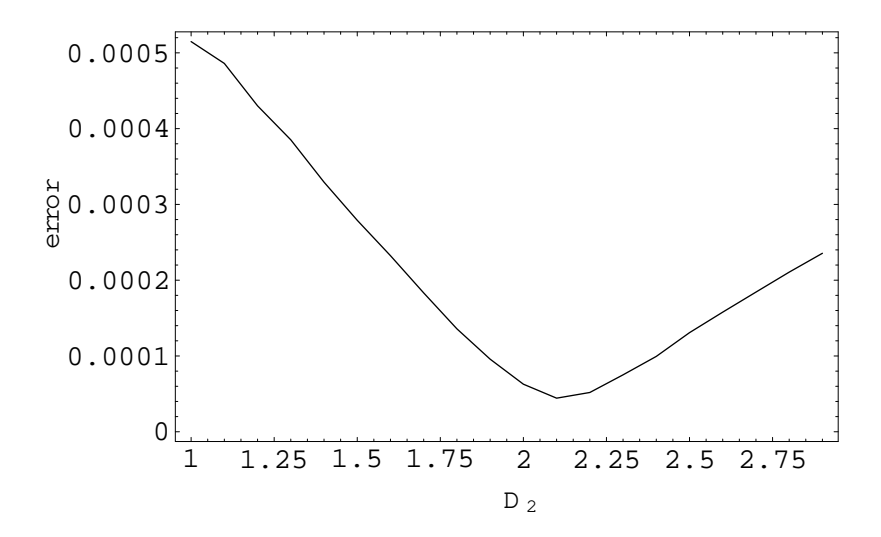


Figure 11: Extracting the scaling dimension  $D_2$  by nite-size scaling, in order to determ in the kinetic term in the elective action of the scale factor.

Our rst step is to determ ine the kinetic term in the elective action of the dynamically triangulated model, and compare it to the term  $a\hat{a}$  of the minisuperspace model (36). We obtain this term by measuring the distribution of differences of adjacent spatial volumes

$$z = \frac{\mathcal{N}_{3}(+1) \quad V N_{3}()\dot{j}}{N_{3}^{1=D_{2}}}; \quad N_{3} = N_{3}() + N_{3}(+1);$$
 (37)

for di erent values of the discrete three-volum e N  $_3$ . A gain, the information we extract is two-fold: we set determine the exponent D  $_2$  from best overlap, and subsequently the overall shape of the universal distribution. In order to maximize the sampled three-volumes, we employ the free boundary conditions described in Sec. 3 above. That is, allow gurations extend over three time steps, = 3, with only a single vertex each at the initial time = 0 and the naltime = 3, and the relevant volumed di erence given by (37), with = 1. From taking measurements at system volumes N° $_4$  = 10, 20, 40, 80 and 160k, we extracted a best value for D  $_2$  by minimizing the failure of the curves to overlap for dierent volumes, using the same method described earlier for the determination of the scaling dimension D  $_{\rm H}$ . The result is illustrated by the curve of F ig. 11 which has its minimum at about 2.12, which we interpret as evidence for D  $_2$  = 2. The overlapping curves

for the volume distributions  $P_{N_3}$  (z) at  $D_2$  = 2 are depicted in Fig. 12. Apart from z-values near zero, the overlap is clearly good. Moreover, the curve is tted very well by a Gaussian  $e^{cz^2}$ , with a positive constant c independent of  $N_3$ .

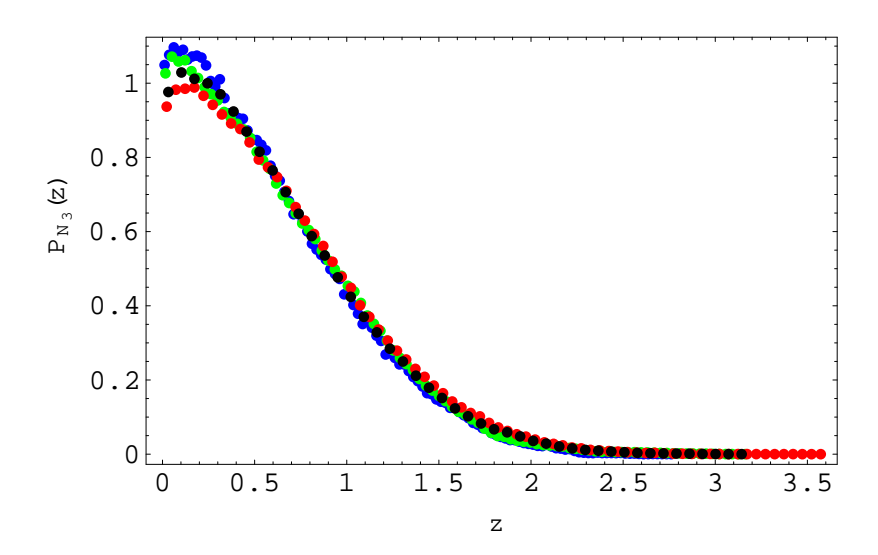


Figure 12: The distribution  $P_{N_3}$  (z) of rescaled volume dierences z between adjacent spatial slices, for three-volumes  $N_3 = 20$ , 40, 80 and 160k.

From estim ating the entropy of spatial geom etries, that is, the num ber N (N  $_3$ ) of three-dim ensional con gurations at given three-volume N  $_3$ , one expects [42] corrections of the form  $\stackrel{\circ}{\text{CN}}_3$ , with 0 < 1,  $\stackrel{\circ}{\text{C}} >$  0, to the exponent  $\stackrel{\circ}{\text{C}} \stackrel{\circ}{\text{C}}$  c (N  $_3$ = ) $^2$ =N  $_3$  in the distribution P  $_{\text{N}_3}$  (z). This leads us to the following form for the Euclidean elective action, valid for large three-volume N  $_3$  ( ),

$$S_{N_4}^e / \sum_{=0}^{X^t} \frac{c_1}{N_3()} - \frac{N_3()}{N_3()}^2 + c_2 N_3() N_3();$$
 (38)

with 0 < 1, and q,  $c_2 > 0$ . In (38), is a Lagrange multiplier to be determined such that

$$X^{t}$$
 $N_{3}() = N_{4};$ 
 $= 0$ 
(39)

Unfortunately it is impossible to measure the precise form of the correction term  $c_2N_3$  directly in a reliable way. However, it is clear from a general scaling of the above action that the only possibility for obtaining the observed scaling law, expressed in terms of the variable  $=N_4^{1=4}$ , is by setting =1=3.10

 $<sup>^{10}\,\</sup>mathrm{In}$  order to correctly reproduce the dynam ics for small three-volume, namely, the stalk

Reverting back to a formulation in terms of the scale factor a(), and by suitable rescaling of and a(), we can now write the electric action of causal dynamical triangulations at xed continuum four-volume  $V_4$  as

$$S_{V_4}^e = \frac{1}{G} d_0 a() \frac{da()}{d} + a() \frac{3}{4}() :$$
 (40)

Again, this expression is valid for su ciently large scale factor, since we have explicitly dropped any reference to the quantum corrections at smalla. Comparing now with (36), the startling conclusion is that we have indeed rederived the Euclidean minisuperspace action. However, here we have done it from rst principles, and up to an overall sign. The strongest evidence so far that the elective action is indeed given by (40) comes from using it as input to create an articial distribution of three-volumes N  $_3$  ( ) [18]. We then evaluate the volume-volume correlator  $c_{N_4}$  (x) of eq. (10) on this ensemble in the same way as we would do for genuine Monte Carlo data. As illustrated in Fig. 13, the matching of this new curve with the previous Monte Carlo results (c.f. Fig. 7) is impressive.

One immediate conclusion is that the collective elect of the dynamical degrees of freedom other than a ( ), which are ignored in minisuperspace models, is to change the sign of the kinetic term for the scale factor (the \global conformal mode") from a divergence of the Euclidean path integral already encountered in dimension 3 [52, 53] and argued for from a continuum point of view in [54]. It provides further evidence that the well-known sicknesses and ambiguities of the Euclidean path integral approach are features of the semiclassical and symmetry-reduced approximations, not shared by a full nonperturbative treatment which is rooted in a causal, Lorentzian formulation.

We have begun an exploration of the consequences of our result for cosm ology and quantum cosm ology. When searching for a physical interpretation, one must keep in mind that the elective action (40) we extracted directly from the computer simulations holds for xed four-volume. Translating between propagators of xed four-volume and xed cosm ological constant requires a further Laplace transformation [18]. Moreover, we are still in the Euclidean sector of the theory, and must Wick-rotate back to obtain physical, Lorentzian results.

Nevertheless, it is exciting to see that the computation of some physical quantities is already within reach: for example, we showed in [18] how to derive the semiclassical wave function of the universe without explicitly performing an inverse Wick rotation. The wave function can be compared directly with those

observed at large times , the function N  $_3^{1=3}$  in (38) with = 1=3 must be replaced by a function of N  $_3$  whose derivative at 0 goes like N  $_3$ , 0, as explained in [18]. A simple choice is the replacement N  $_3^{1=3}$ !  $(1+N_3)^{1=3}$  1.

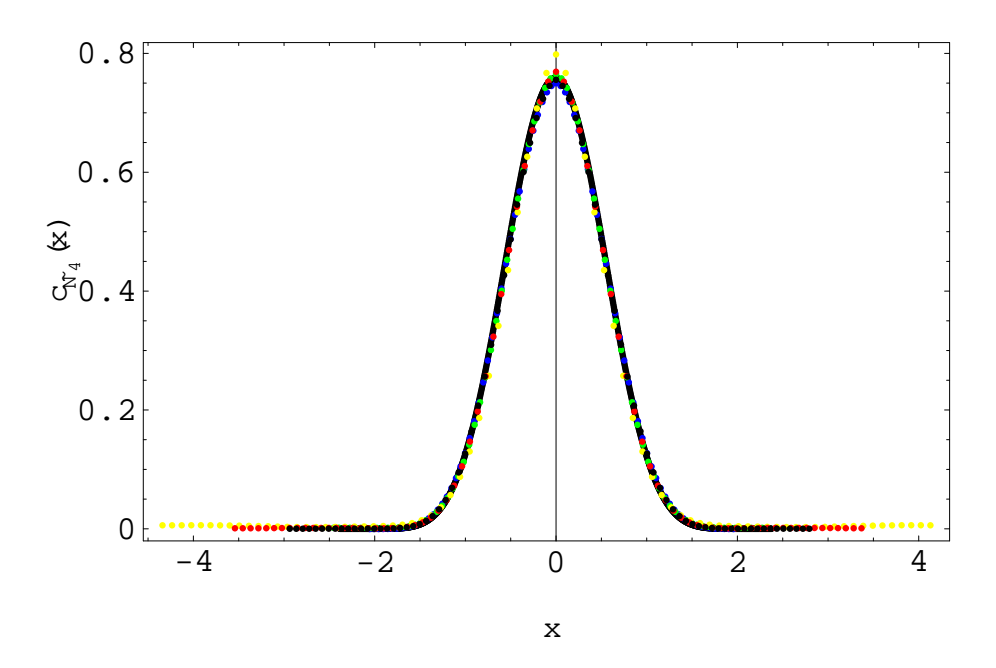


Figure 13: The scaling of the volum e-volum e distribution, as function of the rescaled time variable  $x = (N_4^e)^{1-4}$ , taken from Fig. 7, but now superimposed with the correlator obtained when using the minisuperspace action (40) to generate a distribution of three-geometries (black curve).

arising in standard minisuperspace treatments, like those of Vilenkin [45, 51], Hawking [43, 44] and Linde [46]. To relate to the dynamics of the real universe, especially at very early times, we will need to couple matter to our causal geometries. These issues are currently being investigated and will be reported in the near future.

## 6 Nonclassical structure of the universe: The geometry of spatial slices

Having established that our quantum universe possesses certain classical features at su ciently large scales, we are interested in a more detailed characterization of its geometry. We report in this section on various measurements associated with the geometry of spatial slices = const, and in the next section on that of thick spatial slices", by which we mean geometries of time extension = 1,

which are \sandwiched" between adjacent spatial slices of integer time . Our measurements describe certain invariant geometric properties of the ground state of spacetime, but we make at this stage no attempt to relate them to actual observables that one could go out and measure in the real universe. They will merely serve to illustrate the complexity of the geometric structure and highlight some of its nonclassical features.

Because our universes have a well-de ned global notion of (proper) time , it is relatively straightforward to perform measurements within a slice of constant . We not restrict ourselves to slices S of integer— . Such slices consist entirely of spatial tetrahedra (whose edges are all spacelike). The slices are of the form of spatial interfaces of topology S³ between adjacent sandwiches made out of four-simplices. As we will see, the Hausdor dimension of the slices turns out to be three, as one would have naively expected in a four-dimensional universe. However, the slice does not behave three-dimensionally under diffusion, and we will see that its structure is fractal in a precise sense which will be described below.

### 6.1 Hausdor dimension

Our algorithm for determ ining the Hausdor dimension  $d_h$  of the spatial slices is as follows. From a given S of discrete volume N<sub>3</sub>, we random by pick a tetrahedron  $i_0$ . From  $i_0$ , we move out by one step and obtain n(1) tetrahedra at distance 1 from  $i_0$  (that is, its nearest neighbours). Moving out by a further step, there will be n(2) tetrahedra at distance 2, and so on until all tetrahedra have been visited. The numbers n(r) recorded for each distance r sum up to

$$\Re^{ax}$$
 n (r) = N<sub>3</sub>: (41)

Finally, we measure the average linear extension

$$hri = \frac{1}{N_3} x rn (r)$$
 (42)

of the spatial slice. For a slice of volum e N  $_3$ , this process is repeated N  $_3$ =50 + 1 times with dierent random ly chosen initial tetrahedra. The expectation value hri is then averaged over these measurements. In this way, we obtain for every slice a data pair

fhhrii; 
$$N_3q$$
; (43)

representing one \bare" m easurem ent.

This process is performed for all topatial slices of the geometry, thus collecting to data pairs. We have typically done this for about 1000 dierent spacetime

geom etries, obtaining altogether 1000tm easurement points. The nal results are sorted by their hhrii-value (in practice a continuous variable) and averaged over a sequence of 100 consecutive points. This reduces the number of data points to 10t, which are then displayed on a log-log plot. In the presence of nite-size scaling, we expect them to follow a curve

$$hN_3i(r) / (hri + r_0)^{d_h};$$
 (44)

de ning a spatial Hausdor dimension  $d_h$ . In relation (44), we have included a nite shift  $r_0$  of the linear size r, based on earlier experience with nite-size corrections in the scaling relations [37, 41]. Our results, which show universal behaviour and scaling, are presented in Fig. 14. The shift value  $r_0 = 1:75$  gives

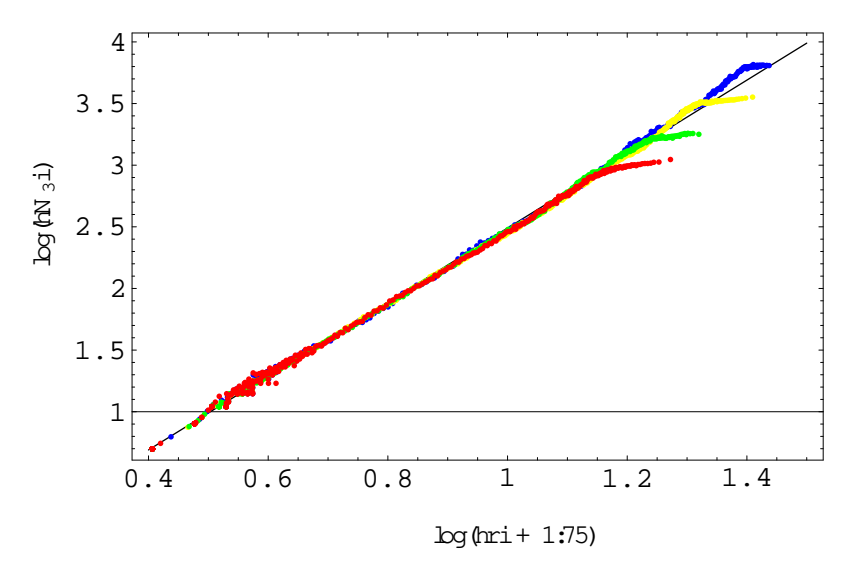


Figure 14: Log-log plot of the average linear geodesic size  $\operatorname{hri}_{N_3}$  versus the three-volum e  $N_3$ , m easured for = 0.4. The straight line corresponds to a Hausdor dimension  $d_h = 3$ . Similar measurements for = 0.5 and 0.6 yield virtually indistiguishable results.

the best linear t. The resulting value of  $d_h$  3 is practically independent of  $\mathfrak{p}$ .

## 6.2 Spectral dim ension

Given the results of the previous sections, one might be tempted to conclude that the geometry of our dynam ically generated ground state  $\sin ply$  is that of a smooth four-dimensional classical spacetime, up to Gaussian uctuations. A more detailed analysis of the geometry of spatial slices makes explicit that this is not so. { We start by measuring the spectral dimension  $d_s$  of the spatial slices

by studying di usion on them . A nalogous to the four-dimensional case described in Sec. 5.2, we choose an initial probability distribution

$$K_{T}(i;i_{0};=0)=_{i:i_{0}}$$
 (45)

on the three-dim ensional triangulation T of the slice S, which is zero everywhere except at a random ly chosen tetrahedron  $i_0$ , and de ne the evolution in discrete time by the rule

$$K_{T}(j;i_{0}; + 1) = \frac{1}{4} {}_{k! \ j} K_{T}(k;i_{0}; );$$
 (46)

where k ! j labels the (four) nearest neighbours of the tetrahedron j. W e m easure the return probability  $P_T$  ( $i_0$ ;  $) = K_T$  ( $i_0$ ;  $i_0$ ; ). The m easurements of the return probabilities are repeated a number of times for each slice S with dierent starting points  $i_0$ , precisely as in the measurement of the Hausdor dimension of S. They are then repeated for independent con gurations (four-dimensional triangulations generated by the M onte C arbo-procedure), again with the same statistics as in the measurement of the Hausdor dimension of the three-dimensional spatial slices. Results are stored for averaged slices with volumes  $N_3 = n$  500 50, because we expect them to depend on the system volume. In this way we do not the average return probability  $P_{N_3}$  () and extract the spectral dimension

$$d_{s}() = 2 \frac{d \log P_{N_{3}}()}{d \log}$$
 (47)

from the logarithm ic derivative exactly as in the four-dimensional di usion process.

The result is displayed in Fig. 15 for even and odd times separately, because of the dierent behaviour of  $P_{\rm N_3}$  () for short evolution times. As can be seen the result is very stable for larger dieusion times and gives  $d_{\rm s}=1:56$  0:1 for the spectral dimension, which is only about half the expected \classical" value!

### 6.3 Critical exponents

The noncanonical value of the spatial spectral dimension shows that the quantum geometry has a nontrivial microstructure, which denitely is not that of a smooth four-dimensional manifold. In fact, we already have come across further evidence of this fact in the measurement of the spacetime spectral dimension which approached the value four only at long distances. One way to obtain an additional characterization of geometries at a xed time is through the functional form of their \entropy" or \number of states" N (N) as function of their discrete volume

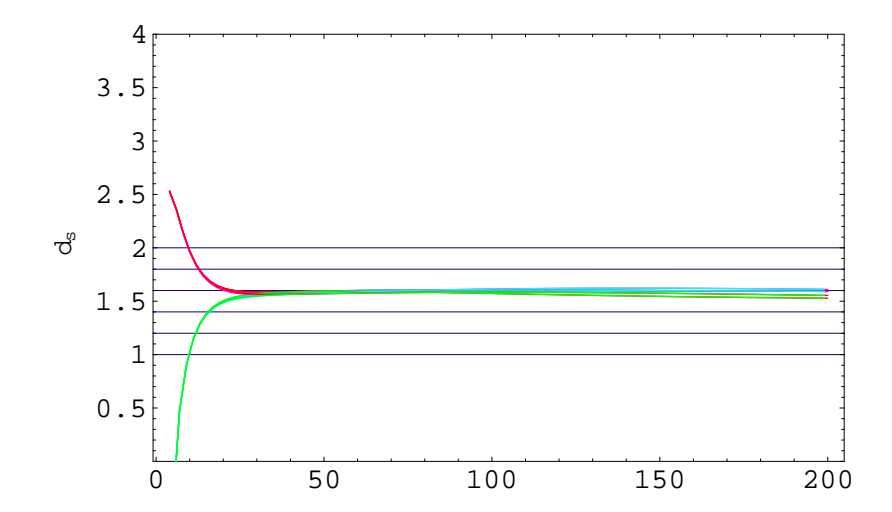


Figure 15: The logarithm ic derivative of the return probability for  $_0 = 2.2$  and = 0.4, and spatial volum es N 3 between 500 and 2000. The m easurem ent was perform ed for a system with  $N_4 = 91.1k$  and t = 40. The increasing and decreasing lines correspond to even and odd tim es, and illustrate the di erent behaviour for short di usion tim es .

N. Two dierent functional forms for the entropy have appeared in previous studies of sim plicial three-dim ensional quantum gravity [42], namely,

$$N (N_3) / N_3^{3+ \text{ str}} e^{0N_3};$$
 (48)  
 $N (N_3) / e^{0N_3 c_1 N_3 +}; < 1;$  (49)

$$N(N_3) / e^{0N_3 c_1 N_3 +}; < 1;$$
 (49)

with a nonuniversal constant  $_{0}$  m easuring the leading exponential growth. The critical exponent str in (48) characterizes the fractal structure of the geometry [56, 57, 58]. The larger the value of str, the more pronounced the tendency for a given three-geometry to develop so-called baby universes 11.

The functional form (49) on the other hand indicates a suppression of baby universes and form ally may be seen as the limit str! 1 of (48). Below we will m eet both functional form s. It is important to understand that the \entropy" N ( $N_3$ ) in (48) and (49) does not merely count the possible three-geometries, but also includes the weight coming from the action: in counting geometries we are

<sup>11</sup> In the present context, a \baby universe" is a part of the three-dimensional spatial triangulation which is connected to the remainder by a \minimal neck". This means that the interface between the triangulated baby universe and the \parent universe" is topologically a sphere and of minimal size. Equivalently, it is given by the surface of a tetrahedron consisting of four triangles. This is easier to visualize in a two-dimensional simplicial manifold where the analogous minimal neck is an S<sup>1</sup> consisting of three edges.

making an importance sampling where the action de nest he probability weight of the geometry. We saw above that the choice of bare coupling constants in the four-dimensional theory determines in which of the dierent phases of the lattice theory we end up. The \entropy" of the spatial geometries at xed time is dierent in the three phases, even if the underlying geometries are identical, and simply given by the space of all (abstract) triangulations of S<sup>3</sup>.

If the functional form of the entropy is given by eq. (48), a convenient way of m easuring the exponent  $_{\rm str}$  is through the distribution of baby universes [57, 58]. Calling B the volume of the baby universe (the number of tetrahedra contained in it) and N $_3$  the total volume of the spatial geometry, we expect a distribution of the form [57, 58]

$$P(x) / x^{2+} str 1 + \frac{C(N_3)}{x} +$$
; (50)

where

$$x = \frac{B}{N_3}$$
 1  $\frac{B}{N_3}$ ; 0 < x < 1=4; (51)

and  $c(N_3)$  / 1=N\_3 is a volume-dependent constant. Relation (50) is expected to hold for su ciently large B. (It was derived under the assumption that the samples of both baby and parent universes have an asymptotic distribution of the form (48).) Since it is very dicult in the present set-up to collect data for any particular xed value of N<sub>3</sub>, we have performed \integrated" measurements to determine  $_{\rm str}$ , by collecting the distribution of the number of baby universes of a given x for various volumes N<sub>3</sub> > 400. Also in this case we expect the distribution of baby universes to follow

$$P(x) / x^{2+} = str + \frac{d}{x} +$$
 (52)

with a constant depending now on the range of three-volumes N  $_3$  over which we have averaged the distribution. The resulting distributions for  $_0$  = 2.2, = 0.4 and total system sizes N  $_4$  = 45.5, 91 and 181k are shown in Fig. 16. Although the measurement is of rather poor quality, and { depending on which range of x is used for the t { the uncertainty in  $_{\rm str}$  rather big, the approximate linearity of the plots strongly suggests that the distribution is indeed dominated by a power law for x. Fitting  $_{\rm str}$  to formula (52), we obtain  $_{\rm str}$  = 0.35 .09.

A nother, seem ingly independent, way of characterizing the short-distance behaviour of the spatial slices S is by m easuring the coordination number of vertices in S, i.e. the number  $n_v$  of spatial tetrahedra sharing a given vertex  $v^{12}$ . In the

 $<sup>^{12}</sup>$ N ote that for a 3d m anifold there is a linear relation between the coordination number of a vertex v and the number of links em erging from v.

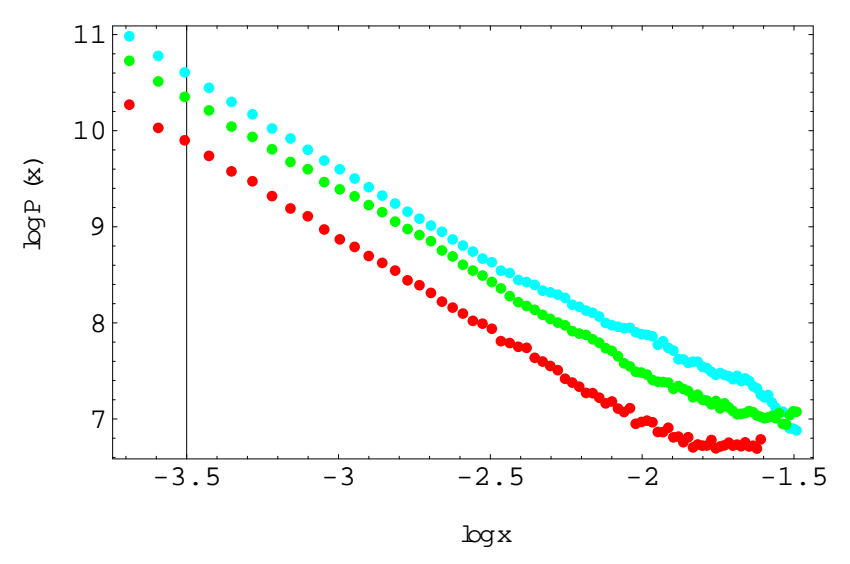


Figure 16: The distribution of the number of baby universes with minimal neck as a function of their rescaled size x, for  $_0 = 2.2$  and  $_0 = 0.4$ . Distributions are normalized by the total number of baby universes in constant-time slices with N  $_3 > 400$ . This number grows with the total spacetime volume N  $_4$ , which is 45.5k (bottom), 91k (middle) and 181k (top curve).

simulations, we observe vertices with relatively high coordination numbers n, and a distribution of n which can be approximated a simple power law

P (n) 
$$/ \frac{1}{(n+n_0)^{1+}}$$
: (53)

As usual, we have included a nite shift  $n_0$  to take into account nite-size e ects. For a three-dim ensional triangulation, n 4 and n m ay take only even values.

Fig. 17 illustrates the distribution of coordination numbers for 4 n 200 m easured for a system with  $_0$  = 2.2, = 0.4, t= 40 and system size N  $_4$  = 181k. The data points have been collected from spatial slices with three-volume N  $_3$  > 500, and can be seen to behave perfectly linearly on the log-log plot. The straight line in Fig. 17 corresponds to a twith = 1.53. In theories of random geometry, this type of power-law behaviour of the vertex coordination number was rst observed in dynamically triangulated bosonic string theory [62]. The value of the exponent extracted from the data by  $^2$ - ts depends slightly on the choice of  $n_0$  and of the cut-o in the data. Our estimate is = 1.53 0.05.

A nother way to determ ine is by studying the distribution of points with the largest coordination number as a function of the spatial volume N $_3$  (or the total number of vertices N $_0$  (N $_3$ ), the two numbers being proportional for the phase of

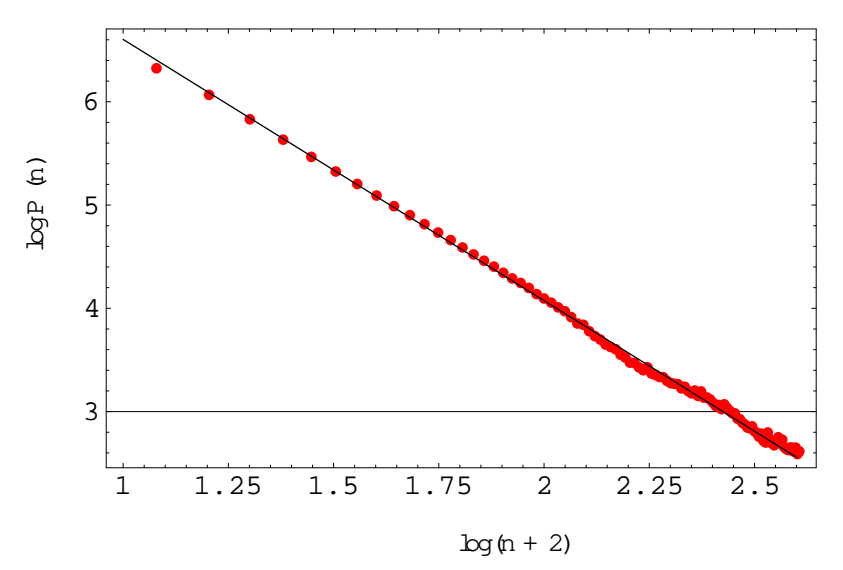


Figure 17: Distribution P (n) of the coordination numbers n of vertices in a three-dimensional spatial slice, for  $_0 = 2.2$  and = 0.4. The straight line represents a numerical to formula (53), with  $n_0 = 2$ .

four-dim ensional gravity we are considering here). One expects a behaviour of the form

$$P (n > n_{max}(T)) / \frac{1}{N_3(T)};$$
 (54)

where  $n_{m \ ax}$  (T) denotes the maximal coordination number for a particular three-dimensional triangulation T. The proportionality (54) is expected to be valid if the distribution P (n) is such that a typical  $n_{m \ ax}$  (T) is so small that it is not in uenced by the fact that the volume N  $_3$  (T) contains only a nite number N  $_0$  (T) of vertices. (Clearly,  $n_{m \ ax}$  (T) cannot be larger than N  $_0$  (T)=2.) Under this assumption the orders  $n_v$  of the N  $_0$  (T) vertices v in T are representative of the distribution P (n). Since there are N  $_0$  (T) of them, the chance of \draw ing" an (abstract) vertex from the distribution P (n) with a coordination number n >  $n_{m \ ax}$  (T) is of the order 1=N  $_0$  (T), which, given N  $_0$  (N  $_3$ ) / N  $_3$ , is equivalent to (54). Consequently, using the scaling (53), we obtain that

$$n_{m ax} (N_3) / N_3^{1=} :$$
 (55)

To check this property, we measure for each surface S the largest coordination numbers in S. Since these uctuate considerably, we measure the average of the three largest values for each S. We then follow a strategy similar to that adopted for the measurement of the Hausdor dimension. Namely, we collect data pairs  $fN_3$ ,  $n_{max}q$ , sort the resulting set by volume  $N_3$  and average over a set of 1000

m easurements. Fig. 18 shows the result in the form of a log-log plot, con m ing the expected linear behaviour. The solid line corresponds to the value

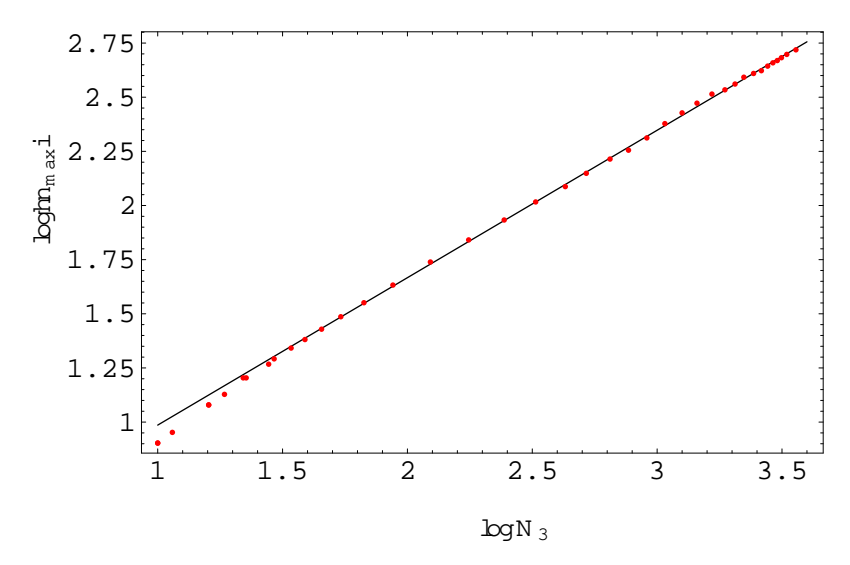


Figure 18: D istribution of the largest coordination number  $n_{max}$  as a function of the spatial volume N<sub>3</sub>, for  $_0 = 22$ ,  $_0 = 0.4$ , t= 40 and N<sub>4</sub> = 91:1k.

$$\frac{1}{-} = 0.681;$$
 (56)

in fair agreement with the previous measurement from smaller correlation numbers, and the tigives 1 = 0.681 .05, translating roughly into = 1.468 0.12. The origin of the uncertainty is the chosen range in the three-volume N<sub>3</sub> taken into account in the tting.

### 6.4 Relation to branched polymers

The above measurements lead to the intriguing conclusion that all the geometric properties of the spatial slices measured so far can be modelled by a particular kind of branched polymers<sup>13</sup>, as we will now go on to explain.

A (planar) branched polymer is an (abstract) one-dimensional polymer which admits arbitrary branching. It is modelled by (abstract) connected planar graphs which contain no loops. As a consequence, cutting any link of such a graph will result in two disconnected graphs. At each vertex an \incom ing" link is allowed

<sup>&</sup>lt;sup>13</sup> In combinatorics, branched polymers are conventionally called rooted trees, where \rooted" means that one link or vertex is marked, and therefore distinguished from the rest.

to  $\$  into n 1  $\$  links with probability p. The statistical model of (rooted) branched polymers is then de ned by the partition function

$$Z_{BP} () = X e^{N} Z_{BP} (N)$$
 (57)

$$Z_{BP} (N) = \begin{pmatrix} X \\ X \\ BP_N \end{pmatrix}; (BP_N) = \begin{pmatrix} Y^N \\ p_n; \end{pmatrix}$$
 (58)

where the sum mation is over all branched polymers with N vertices, and the weight (BP) is the product of the branching probabilities. One can also embed the abstract branched polymers in a target space, either a lattice or R<sup>d</sup>. In the latter case, it is convenient to work with a quadratic action  $(x_u \ x_v)^2$  for pairs of nearest-neighbour vertices u and v with coordinates  $x_u$  and  $x_v$ , and perform an additional integration over the target-space coordinates in the partition function.

The fractal properties of branched polymers are well understood. The leading behaviour for large N is an analogue of eq. (48), namely,

$$Z_{BP} (N) N^2 e^{0N};$$
 (59)

where can take a range of real values, depending on the branching probability  $p_n$ . The intrinsic Hausdor dimension  $d_h^{(in)}$  of branched polymers with > 0 is [59, 60, 61]

$$d_h^{(in)} = \frac{1}{i}$$
 (60)

with spectral dimension given by [38, 39]

$$d_s = \frac{2}{1+}$$
: (61)

We note that formulas (60) and (61) already provide a close match with our data if we identify with the str of the simulations. As we will see, there is indeed a concrete branched-polymer model which has the -value we have observed. In regularized bosonic string theory one is naturally led to studying branched polymers with branching weight [62]

$$p_n = \frac{1}{n}$$
 for n 1: (62)

Generically, the value of for a given is

() = 1=2 for 1;  
() = 1 for 
$$1 < 3$$
; (63)

 $<sup>^{14}</sup>$ The dierence between the power 2 in eq. 69) and 3 of eq. (48) arises because of the use of rooted branched polymers, which gives rise to an extra factor of N.

which does not cover the —range we are interested in . However, if the partition function satis es a certain technical condition 15, the relations (63) are changed to

$$() = (1) = \text{for } 1 < < 2$$
  
 $() = 1 = 2 \qquad \text{for } 2$ 
(65)

([61], and see [16] for a detailed discussion). While the associated condition (64) seems rather articial from the perspective of branched polymers, it appears in a natural way if the branched polymers emerge as a limit of higher-dimensional models like noncritical strings with central charge c > 1. As a matter of fact, the generic value of in this case is 1/3 [60]. Sum marizing the critical exponents for this particular class of branched polymers,

$$= \frac{1}{3}; \quad d_h^{(in)} = 3; \quad d_s = \frac{3}{2}; \qquad = \frac{3}{2}; \tag{66}$$

we see that within the measuring accuracy, they are precisely the numbers characterizing the spatial geometries of causal dynamical triangulations at constant time. Although the vertex order  $n_{\rm v}$  of our three-dimensional triangulations has a priori nothing to do with the branching of polymers, the above results are a strong hint that there electively is such a connection. While this cone measure earlier assertion that the geometry of the spatial slices behaves very nonclassically, it opens the exciting possibility that quantum gravity as described by this model may be amenable to analytic approximations, precisely as was the case in the study of noncritical strings with c>1 [60].

# 7 Nonclassical structure of the universe: The geometry of \thick" spatial slices

A nother substructure of spacetim e whose geom etry can be investigated straightforwardly are what we shall call \thick" spatial slices, namely, the sandwiches of geometry contained in between two adjacent spatial slices of integer times and +1, with topology I  $\mathring{S}$ . As illustrated in Fig. 1, they are made up of four-simplices of types (4,1) and (3,2) and their time-reversed counterparts (1,4) and (2,3). Because of their nite time extension, one might expect the geometry of the thick slices to behave more \classically", and this is indeed corroborated

$$\frac{dZ_{BP}()}{d} < 0 \text{ for } > 0; \qquad \frac{dZ_{BP}()}{d} = 0 = 1;$$
 (64)

which is naturally satis ed for some branched polymer models coming from noncritical string theory [60].

<sup>&</sup>lt;sup>15</sup>For (65) to hold one needs

by our simulations, which include a measurement of the Hausdor and spectral dimension of the thick slices.

A convenient way to represent a sandwich geometry is by considering the three-dim ensional piecew ise at geom etry that results by cutting the thick slice + 1=2. The analogous procedure in one dimension less, which is easier to visualize, gives a generalized two-dimensional triangulation consisting of triangles and squares [52, 31, 30]. The triangles are the intersection surfaces of (3,1)- and (1,3)-tetrahedra, and the squares those of (2,2)-tetrahedra. In one dim ension higher, the fundam ental building blocks are no longer tetrahedra but four-sim plices. Consequently, the intersection patterns are three-dimensional at building blocks, namely, spatial tetrahedra from slicing the (4,1)-and (1,4)sim plices, and spatial triangular prisms from slicing the (3,2)-and (2,3)-sim plices. In order to distinguish between a tetrahedron that comes from cutting a (4,1)simplex from one associated with an upside-down, (1,4)-simplex, one colour-codes the links of the intersection hypersurface into red and blue, say. The red links are those that will be \shrunk away" when the constant-time surface approaches the integer-time + 1, and similarly the blue links will disappear as the hypersurface is moved towards time . As a result, the tetrahedra have all links of one colour, whereas the prisms are always bi-coloured (see also [20]). Note that the average spatial volume in terms of counting three-dimensional building blocks is larger (by a factor of about 2.5) at slices of half-integer time, because { unlike at integer tim es { all four-sim plices between and + 1 contribute to the counting.

#### 7.1 The Hausdor dimension

To determ ine the Hausdor dimension  $d_H$  of the thick slices, we pick a random four-simplex from such a slice, or, equivalently, a random three-dimensional building block from the corresponding intersection pattern at half-integer time. Continuing in this three-dimensional representation of the slice geometry, we proceed exactly as we did when measuring the Hausdor dimension  $d_h$  of the spatial slices at integer—. Starting from the random ly chosen initial three-dimensional building block, we move out, one step at a time, to the nearest neighbours at distance r, from the previous set of building blocks at distance r—1. In terms of four-simplices, this means we never move out to simplices earlier than—or later than—+1, that is, by denition we never leave the thick slice. At each step, we keep track of the number n (r) of building blocks, whose sum is equal to the total slice volume N,

and which enables us to compute the average linear size

$$hri = \frac{1}{N} X rn (r)$$
 (68)

of the thick slice. For a given slice of volume N , this process is then repeated N  $_4\!=\!100+1$  times with random by chosen initial building blocks. The average size hri is again averaged over this set and the data pair fhhrii; N g stored. U sing the same procedure as described following formula (43) above, we extract the H ausdor dimension  $d_{\rm H}$  from the relation

$$N_4 / (hri + r_0)^{d_H};$$
 (69)

with a nite constant  $r_0$  taking into account nite-size corrections. The results are presented in Fig. 19 in the form of a log-log plot. The straight line corresponds

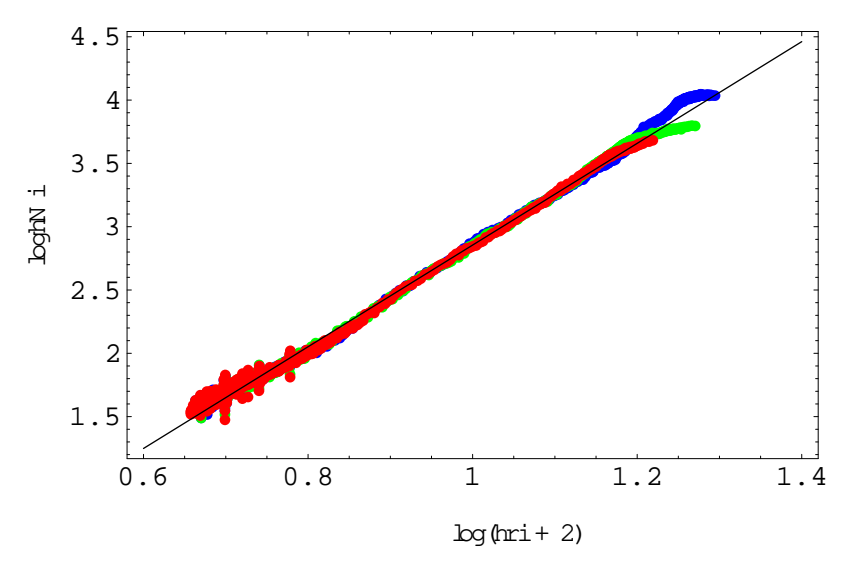


Figure 19: Log-log plot of the average linear geodesic size  $hri_N$  versus the volum e N of a thick slice. The straight line corresponds to a Hausdor dimension  $d_H = 4$ .

to  $d_H$  = 4, and the best tted value is  $d_H$  = 4.01 0.05. M easurements were performed on spacetimes with total size  $N_4$  = 20, 40 and 80k, at  $_0$  = 2.2, = 0.6 and t = 80. { We conclude that the transition from a genuine constant-time slice to a thick slice adds one extra dimension to the Hausdor dimension { the thickened slice already \feels" some aspects of the four-dimensionality of the full spacetime. Note that this would not be true for a thick slice of a classical, regular lattice, whose Hausdor dimension would be the same as that of a \thin" slice. The likely mechanism for the dimensional increase in the triangulations is the appearance of \short-cuts" between two tetrahedral building blocks, say, once one moves slightly away from a slice of integer— .

#### 7.2 The spectral dim ension

Next, we turn to the spectral dimension  $d_{\rm S}$  of the thick slices. When adapting our earlier measurement of the spectral dimension  $d_{\rm S}$  of spatial slices, we have to take into account that the tetrahedral building blocks in the three-dimensional intersection pattern at half-integer have four neighbours, whereas the prisms have ve. We start from an initial probability distribution

$$K_{T}(i; i_{0}; = 0) = i_{1}i_{0}$$
 (70)

concentrated at a random ly chosen three-dimensional building block with label  $i_0$  in the three-dimensional \triangulation" T (consisting of tetrahedra and triangular prisms), and de ne the evolution process by

$$K_{T}(j;i_{0}; + 1) = X_{k! j} \frac{1}{g_{k}} K_{T}(k;i_{0}; );$$
 (71)

where  $g_i$  denotes the number of neighbours of building block i, and k! j are the nearest neighbours of the \sim plex" j (which can now also be a prism). By construction, the total probability

$$X K_{T}(i;i_{0};) = 1 (72)$$

is conserved. As before, we measure the return probability K  $_{\rm T}$  (i\_0; i\_0; ). After the appropriate averaging over initial points i\_0 and triangulations T we obtain the quantum return probability  $P_{\rm N}$  ( ) as a function of the number of building blocks N in the triangulations T (we keep the number N approximately constant in the triangulations included in the average). The expected behaviour

$$P_N$$
 ( ) /  $d_{S}=2$  + nite-size corrections (73)

de nesa spectral dim ension  $d_S$ , which in general will be dierent from the spectral dim ension  $d_S$  determined for the constant-time slices. The value of  $d_S$  is extracted by measuring the logarithmic derivative of  $P_N$  () as a function of the evolution time,

$$d_{S}() = 2 \frac{d \log P_{N}()}{d \log}$$
: (74)

The results of our measurements are displayed separately for even and odd times in Fig. 20, since the behaviour of  $P_{\rm N}$  ( ) is dierent for very small (as already observed in our previous measurements of spectral dimensions). As seen in the gure, beyond small we do not not the perfect constant logarithmic derivative observed earlier for the \thin" slices at integer time. If we nevertheless treat

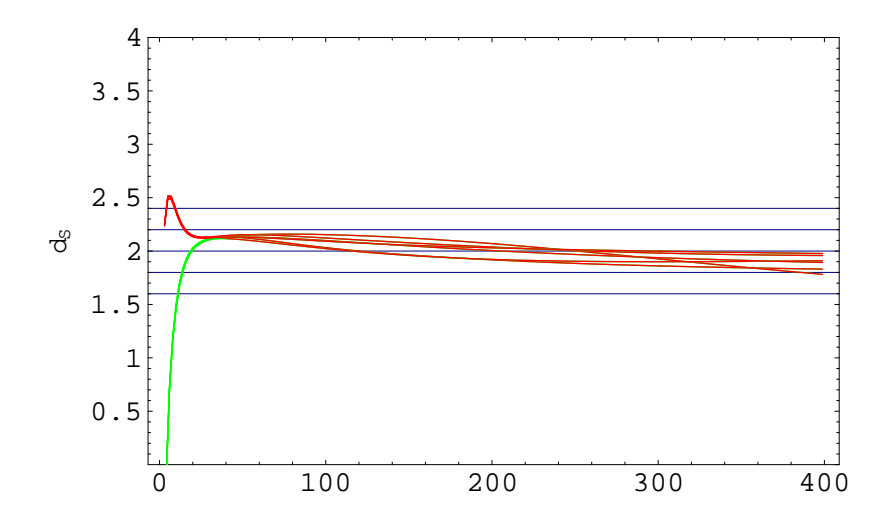


Figure 20: The logarithm ic derivative of the return probability for  $_0$  = 2:2 and = 0:6 and thick slices of volumes N between 900 and 2000. The measurement was performed for a system with N  $_4$  = 161k and t= 80. Curves extrapolating between even evolution times decrease rapidly at small , whereas curves of odd times stay above  $d_S$  = 2 at small times.

the output curves as constants and take their mean value as representative of the logarithm ic derivative  $d_{\rm S}$  (assuming it is —independent), we obtain  $d_{\rm S}=2:0-0:2$ . A lthough it lies above the value  $d_{\rm S}$  for the spectral dimension of the spatial slices, this dimensionality is still highly nonclassical, and rejects the presence of some intermediate regime between a purely spatial and a purely spacetime geometry.

# 7.3 Baby universes

To further characterize the geometry of thick slices, we also looked into its baby universe structure. M inim alnecks can take the form of either four triangles, form ing the surface of a tetrahedron, or of two triangles and three squares, form ing the surface of a triangular prism (of course, without an interior tetrahedron or prism being located there). It turns out that the four-dimensional manifold constraints, which ensure that the four-sim plices are glued in a way that results in a sim plicial manifold, in pose severe restrictions on the types of baby universes with minimal necks that can occur. For a tetrahedral minimal neck, the baby universe which branches of there can only contain building blocks which are tetrahedra of the

 $<sup>^{16}</sup>$ A nalogousm anifold conditions for intersection graphs in three-dim ensionals implicial spacetimes were formulated in [31].

sam e colour. M inim al necks of the form of a prism cannot occur altogether. We attempted to measure the distribution of \monochrome" tetrahedral baby universes, but found them to be small in size, within a range practically independent of the slice volume N. We did not check for baby universes with larger necks. Our tentative conclusion is that the microscopic structure of the thick slices is more regular than that of the genuine spatial slices of xed constant time.

It is tempting to conjecture that the absence of baby universes means that the entropy function N (V) for the thick spatial slices has the functional form (49) rather than (48), which was the form observed for the thin spatial slices at xed integer time. As mentioned in Sec. 6.3, the entropy behaviour (49) signals an almost complete suppression of baby universes. Moreoever, if the exponent in eq. (49) was equal to 1/3, it would to neatly with the observation that the elective macroscopic action (40), which reproduces so well the macroscopic four-dimensional features we observe in the simulations, does contain the characteristic linear term in the scale factor a () (corresponding to a factor  $V_3^{1=3}$  () in terms of the continuum three-volume). It would also be in line with our expectation that the structure of the thick spatial slices, rather than that of the thin slices at xed time should relate most directly to the global four-dimensional structure.

# 8 Sum m ary and outlook

This paper describes the currently known geom etric properties of the quantum universe generated by the method of causal dynam ical triangulations, as well as the general phase structure of the underlying statistical model of four-dimensional random geometries. The main results are as follows. An extended quantum universe exists in one of the three observed phases of the model, which occurs for su ciently large values of the bare Newton's constant G and of the asymmetry, which quanties the nite relative length scale between the time and spatial directions. In the two other observed phases, the universe disintegrates into a rapid succession of spatial slices of vanishing and nonvanishing spatial volume (small G), or collapses in the time direction to a universe that only exists for an in nitesimal moment in time (large G, vanishing or small). In either of these two cases, no macroscopically extended spacetime geometry is obtained.

By measuring the (Euclidean) geometry of the dynamically generated quantum spacetime<sup>17</sup> in the remaining phase, in which the universe appears to be extended in space and time, we collected strong evidence that it behaves as a four-dimensional quantity on large scales. First, nite-size scaling of the volume-volume correlator for spatial slices is observed when the time variable is rescaled

 $<sup>^{17}</sup>$ Since our universe is a weighted quantum superposition of geom etries, all \m easurem ents" refer to expectation values of geom etric operators in the quantum ground state.

by the fourth root of the discrete four-volume, eq.(11), within measuring accuracy. Second, the large-scale spectral dimension of the universe, determined from a di usion process on the quantum ensemble of geometries, is compatible with the value 4.

The dynamical derivation of the correct classical result for the dimension from a completely nonperturbative path-integral setting provides a considerable boost to our e orts to construct a theory of quantum gravity by the method of causal dynam ical triangulations. Furtherm ore, we were able to show that the universe possesses other features of classical geom etry at su ciently large scales. Nam ely, using the four-dimensionality at large scales, we derived an elective Euclidean action for the scale factor of the universe (equivalently, the volume of its spatial slices). For the case of xed spacetime volume, this action coincides up to an overall sign with a simple minisuperspace action frequently used in quantum cosm ology. Again, we believe that this is a highly nontrivial and very exciting result. It has already enabled us to derive a \wave function of the universe" from rst principles [18]. The change in sign of the action in plies that the Euclidean sector of our quantum gravity model is well-de ned. This is a welcome result since, unlike in standard quantum cosmology, no ad hoc cure is needed to deal with a conformal kinetic term that renders the action unbounded below. Some care is required in interpreting it, since we still need to perform an inverse W ick rotation to get back to the physical, Lorentzian sector of the theory. A detailed discussion will appear elsewhere.

Returning to the analysis of the quantum geometry of our universe, we gained further insights by performing measurements of a more local nature by looking at the intrinsic geometry of \thin" and \thick" spatial slices. A thin slice is by de nition a spatial geometry at xed integer time somewhere inside a universe, and a thick slice a piece of spacetime contained between two adjacent thin slices. We found that in general them easured observables exhibit nonclassical behaviour, in the sense that dynamically determined dimensionalities of the slices do not coincide with the values one would have expected naively for the corresponding submanifolds of a classical four-dimensional spacetime. This result is not in contradiction with the four-dimensional behaviour of the universe at large scales, but underscores the fact that the local geometry of the quantum spacetime has highly nonclassical features.

We found that the measured Hausdor dimension of thin slices comes out as 3 with good accuracy, but that the spectral dimension is only around 15! By making additional measurements of the distributions of vertex coordination numbers and of baby universes in the thin slices we were able to show that

<sup>&</sup>lt;sup>18</sup>One should keep in m ind that slices of constant time are in noway physically distinguished in a theory of pure gravity, and their geometric properties therefore not directly related to physical observables.

the entire set of parameters is matched by the critical exponents of a particular class of branched polymers, potentially opening a new window to an analytic investigation of quantum spacetime.

The thick slices were found to have Hausdor dimension 4 within measuring accuracy, and a spectral dimension of around 2. This, and the apparent absence of baby universes of appreciable size indicate that the geometry of the thick slices represents a genuinely intermediate case between that of the thin slices and of the full spacetime. In particular, their geometry { although far from being classical { seems to be more regular than that of the thin slices.

Them ost localm easurement of quantum geometry so far is that of the spectral dimension of spacetime at short distances, which provides another quantitative measure of the nonclassicality of geometry. As we have seen, the spectral dimension changes smoothly from about 4 on large scales to about 2 on small scales. Not only does this (to our knowledge) constitute the rst dynamical derivation of a scale-dependent dimension in quantum gravity, but it may also provide a natural short-distance cut-o by which the nonperturbative formulation evades the ultra-violet in nities of perturbative quantum gravity.

In sum mary, what emerges from our form ulation of nonperturbative quantum gravity as a continuum limit of causal dynamical triangulations is a compelling and rather concrete geometric picture of quantum spacetime. Quantum spacetime possesses a number of large-scale properties expected of a four-dimensional classical universe, but at the same time exhibits a nonclassical and nonsmooth behaviour microscopically, due to large quantum uctuations of the geometry at small scales. These uctuations \conspire" to create a quantum geometry that is e ectively two-dimensional at short distances.

O fcourse, our large-scale measurements of geometry so far do not characterize the classical properties of our quantum spacetime completely, and further work is under way to determine its large-scale curvature properties, and check that Newton's inverse square law can be recovered in an appropriate limit (see [63] for related previous attempts). Having established the existence of a meaningful classical limit opens the door to the ultimate subject of our interest, the quantum behaviour of the local gravitational degrees of freedom. On the one hand, together with appropriate matter degrees of freedom, they should be able to describe the quantum behaviour of the very early universe, which may have left an imprint on the cosmic microwave background radiation we observe today. On the other hand, they will characterize the uctuations around a large-scale classical background, like that of our present universe, leading to quantiable deviations from the predictions of classical relativity.

## R eferences

- [1] A. Bonanno and M. Reuter: Proper time ow equation for gravity,, JHEP 0502 (2005) 035 [hep-th/0410191].
  - M. Reuter and H. Weyer: Running Newton constant, improved gravitational actions, and galaxy rotation curves, Phys. Rev. D 70 (2004) 124028 [hep-th/0410117].
  - M.Reuter and F.Saueressig: A class of nonlocal truncations in quantum Einstein gravity and its renormalization group behavior, Phys. Rev. D 66 (2002) 125001 [hep-th/0206145].
  - Renormalization group ow of quantum gravity in the Einstein-Hilbert truncation, Phys. Rev. D 65 (2002) 065016 [hep-th/0110054].
- [2] T. Thiemann: Lectures on loop quantum gravity, Lect. Notes Phys. 631 (2003) 41 [gr-qc/0210094].
- [3] C.Rovelli: Quantum gravity, Cambridge University Press, Cambridge, UK, 2004.
- [4] H.Nicolai, K.Peeters and M.Zamaklar: Loop quantum gravity: An outside view, [hep-th/0501114].
- [5] A. Perez: Spin foam models for quantum gravity, Class. Quant. Grav. 20 (2003) R43-R104, [gr-qc/0301113].
- [6] J. Ambj m and R. Loll: Non-perturbative Lorentzian quantum gravity, causality and topology change, Nucl. Phys. B 536 (1998) 407-434 [hep-th/9805108].
- [7] J. Ambj m, J. Jurkiewicz and R. Loll: A nonperturbative Lorentzian path integral for gravity, Phys. Rev. Lett. 85 (2000) 924-927 [hep-th/0002050].
- [8] J.Ambj m, J.Jurkiewicz and R.Loll: Dynamically triangulating Lorentzian quantum gravity, Nucl. Phys. B 610 (2001) 347–382 [hep-th/0105267].
- [9] J.Ambj m and J.Jurkiew icz: Four-dim ensionalsim plicial quantum gravity, Phys. Lett. B 278 (1992) 42-50.
- [10] J.Ambj m and J.Jurkiewicz: Scaling in four-dimensional quantum gravity, Nucl. Phys. B 451 (1995) 643-676 [hep-th/9503006].
- [11] P. Bialas, Z. Burda, A. Krzywicki and B. Petersson: Focusing on the xed point of 4d simplicial gravity, Nucl. Phys. B 472 (1996) 293-308 [hep-lat/9601024].

- [12] P.Bialas, Z.Burda, B.Petersson and J.Tabaczek: Appearance of mother universe and singular vertices in random geometries, Nucl. Phys. B 495 (1997) 463-476 [hep-lat/9608030].
- [13] S. Catterall, J.B. Kogut and R. Renken: Phase structure of four-dimensional simplicial quantum gravity, Phys. Lett. B 328 (1994) 277-283 [hep-lat/9401026].
- [14] S.Catterall, R.Renken and J.B.Kogut: Singular structure in 4D simplicial gravity, Phys.Lett.B 416 (1998) 274-280 [hep-lat/9709007].
- [15] B.V. de Bakker and J. Sm it: Curvature and scaling in 4-d dynam ical triangulation, Nucl. Phys. B 439 (1995) 239-258 [hep-lat/9407014].
- [16] J. Ambj m, B. Durhuus and T. Jonsson: Quantum geometry, Cambridge M onographs on M athematical Physics, Cambridge University Press, Cambridge, UK, 1997.
- [17] J.Ambj m, J.Jurkiewicz and R.Loll: Emergence of a 4D world from causal quantum gravity, Phys. Rev. Lett. 93 (2004) 131301 [hep-th/0404156].
- [18] J. Ambj m, J. Jurkiewicz and R. Loll: Semiclassical universe from rst principles, Phys. Lett. B 607 (2005) 205–213 [hep-th/0411152].
- [19] J. Ambj m, J. Jurkiewicz and R. Loll: Spectral dimension of the universe, preprint Utrecht, M ay 2005 [hep-th/0505113].
- [20] B.D ittrich and R.Loll: Counting a black hole in Lorentzian product triangulations, preprint U trecht, to appear.
- [21] JW .A lexander: The combinatorial theory of complexes, Ann. Mat. 31 (1930) 292.
- [22] U. Pachner: Bistellare Aquivalenz kombinatorischer Mannigfaltigkeiten, Arch. Math. 30 (1978) 89.
- [23] M. Gross and S. Varsted: Elementary moves and ergodity in d-dimensional simplicial quantum gravity, Nucl. Phys. B 378 (1992) 367-380.
- [24] J. Ambj m and S. Varsted: Three-dimensional simplicial quantum gravity, Nucl. Phys. B 373 (1992) 557-580.
- [25] J.Ambj m, B.Durhuus and T.Jonsson: Statisticalm echanics of paths with curvature dependent action, J.Phys. A 21 (1988) 981-1000.

- [26] S.W einberg: Ultraviolet divergences in quantum theories of gravitation, in General relativity: Einstein centenary survey, eds. S.W. Hawking and W. Israel, Cambridge University Press, Cambridge, U.K. (1979) 790-831.
- [27] H. Kawai, Y. Kitazawa and M. Ninomiya: Renormalizability of quantum gravity near two dimensions, Nucl. Phys. B 467 (1996) 313-331 [hep-th/9511217].

  Ultraviolet stable xed point and scaling relations in (2+epsilon)-dimensional quantum gravity, Nucl. Phys. B 404 (1993) 684-716 [hep-th/9303123].

  Scaling exponents in quantum gravity near two-dimensions, Nucl. Phys. B

393 (1993) 280-300 [hep-th/9206081].

- H.Kawai and M.Ninomiya: Renormalization group and quantum gravity, Nucl. Phys. B 336 (1990) 115-145.
- [28] H.W. Hamber: On the gravitational scaling dimensions, Phys. Rev. D 61 (2000) 124008 [hep-th/9912246].

  Phases of simplicial quantum gravity in four-dimensions: Estimates for the critical exponents, Nucl. Phys. B 400 (1993) 347-389.
- [29] M E.Agishtein and A.A.Migdal: Critical behavior of dynamically triangulated quantum gravity in four-dimensions, Nucl. Phys. B 385 (1992) 395-412 [hep-lat/9204004].
- [30] J.Ambj m, J.Jurkiew icz and R.Loll: Renormalization of 3d quantum gravity from matrix models, Phys. Lett. B 581 (2004) 255-262 [hep-th/0307263].
- [31] J. Ambj m, J. Jurkiewicz, R. Loll and G. Vernizzi: Lorentzian 3d gravity with worm holes via matrix models, JHEP 0109 (2001) 022 [hep-th/0106082].
- [32] S. Catterall, G. Thorleifsson, J.B. Kogut and R. Renken: Singular vertices and the triangulation space of the D-sphere, Nucl. Phys. B 468 (1996) 263-276 [hep-lat/9512012].
- [33] M E J. Newman and G J. Barkema: Monte Carlo methods in statistical physics, Oxford University Press, Oxford, UK, 1999.
- [34] H.Kawai, N.Kawamoto, T.Mogamiand Y.Watabiki: Transfer matrix formalism for two-dimensional quantum gravity and fractal structures of spacetime, Phys. Lett. B 306 (1993) 19-26 [hep-th/9302133].
- [35] J.Ambj m and Y.W atabiki: Scaling in quantum gravity, Nucl. Phys. B 445 (1995) 129-144 [hep-th/9501049].

- [36] S.Catterall, G.Thorleifsson, M.J.Bowick and V.John: Scaling and the fractal geometry of two-dimensional quantum gravity, Phys. Lett. B. 354 (1995) 58-68 [hep-lat/9504009].
- [37] J. Ambj m, J. Jurkiewicz and Y. Watabiki: On the fractal structure of two-dimensional quantum gravity, Nucl. Phys. B 454 (1995) 313-342 [hep-lat/9507014].
- [38] T. Jonsson and J.F. W heater: The spectral dimension of the branched polymer phase of two-dimensional quantum gravity, Nucl. Phys. B 515 (1998) 549-574 [hep-lat/9710024].
- [39] J.Ambj m, D.Boulatov, J.L.N ielsen, J.Rolfand Y.W atabiki: The spectral dimension of 2D quantum gravity, JHEP 9802 (1998) 010 [hep-th/9801099].
- [40] J.Ambj m, K. N. Anagnostopoulos, T. Ichihara, L. Jensen and Y. W. atabiki: Quantum geometry and diusion, JHEP 9811 (1998) 022 [hep-lat/9808027].
- [41] J. Ambj m and K.N. Anagnostopoulos: Quantum geometry of 2D gravity coupled to unitary matter, Nucl. Phys. B 497 (1997) 445-478 [hep-lat/9701006].
- [42] J. Ambj m, D. V. Boulatov, A. Krzywicki and S. Varsted: The vacuum in three-dimensional simplicial quantum gravity, Phys. Lett. B 276 (1992) 432-436;
- [43] JB. Hartle and SW. Hawking: Wave function of the universe, Phys. Rev. D 28 (1983) 2960-2975.
- [44] G. W. G. ibbons and S. W. Hawking: Euclidean quantum gravity, World Scientic, Singapore, 1993.
- [45] A.Vilenkin: Creation of universes from nothing, Phys. Lett. B 117 (1982) 25–28; Quantum creation of universes, Phys. Rev. D 30 (1984) 509–511.
- [46] A.D. Linde: Quantum creation of the in ationary universe, Lett. Nuovo Cim. 39 (1984) 401-405.
- [47] V.A.Rubakov: Quantum mechanics in the tunneling universe, Phys. Lett. B 148 (1984) 280-286.
- [48] J.J.Halliwelland J.Louko: Steepest descent contours in the path integral approach to quantum cosmology. 1. The de Sitter m in isuperspace model, Phys. Rev. D 39 (1989) 2206–2215.

- [49] J.J.Halliwelland J.B.Hartle: Integration contours for the no boundary wave function of the universe, Phys. Rev. D 41 (1990) 1815-1834.
- [50] A. Vilenkin: Approaches to quantum cosmology, Phys. Rev. D 50 (1994) 2581-2594 [gr-qc/9403010].
- [51] A. Vilenkin: Quantum cosmology and eternal in ation, in \The fiture of theoretical physics and cosmology", eds. G. W. G. ibbons, E. P. S. Shellard and S. J. Rankin, Cambridge University Press (2003) 649-666 [gr-qc/0204061].
- [52] J.Ambj m, J.Jurkiew icz and R.Loll: Nonperturbative 3-d Lorentzian quantum gravity, Phys. Rev. D 64 (2001) 044011 [hep-th/0011276].
- [53] J. Ambjm, A. Dasgupta, J. Jurkiewicz and R. Loll: A Lorentzian cure for Euclidean troubles, Nucl. Phys. Proc. Suppl. 106 (2002) 977-979 [hep-th/0201104].
- [54] A.Dasgupta and R.Loll: A proper-time cure for the conformal sickness in quantum gravity, Nucl. Phys. B 606 (2001) 357-379 [hep-th/0103186].
- [55] J. Ambj m, K. Anagnostopoulos, T. Ichihara, L. Jensen, N. Kawam oto, Y. Watabiki and K. Yotsuji: The quantum space-time of c = -2 gravity, Nucl. Phys. B 511 (1998) 673-710 [hep-lat/9706009].
- [56] S. Jain and S.D. Mathur: World sheet geometry and baby universes in 2-D quantum gravity, Phys. Lett. B 286 (1992) 239-246 [hep-th/9204017].
- [57] J. Ambj m, S. Jain and G. Thorleifsson: Baby universes in 2-d quantum gravity, Phys. Lett. B 307 (1993) 34-39 [hep-th/9303149].
- [58] J. Ambj m, S. Jain, J. Jurkiewicz and C.F. Kristjansen: Observing 4-d baby universes in quantum gravity, Phys. Lett. B 305 (1993) 208-213 [hep-th/9303041].
  J. Ambj m, P. Bialas, J. Jurkiewicz, Z. Burda and B. Petersson: E ective sampling of random surfaces by baby universe surgery, Phys. Lett. B 325
- [59] J.Ambj m, B.Durhuus and T.Jonsson: Sum m ing over all genera for d > 1: a toy model, Phys. Lett. B 244 (1990) 403-412.

(1994) 337-346 [hep-lat/9401022].

[60] J.Ambj m, B.Durhuus and T.Jonsson: A solvable 2-d gravity model with gamma > 0, Mod. Phys. Lett. A 9 (1994) 1221-1228 [hep-th/9401137].
J.Ambj m, B.Durhuus, T.Jonsson and G.Thorleifsson: Matter elds with c > 1 coupled to 2-d gravity, Nucl. Phys. B 398 (1993) 568-592 [hep-th/9208030].

- [61] J. Jurkiewicz and A. Krzywicki: Branched polymers with loops, Phys. Lett. B 392 (1997) 291-297 [hep-th/9610052].
- [62] J. Ambj m, B. Durhuus and J. Frohlich: The appearance of critical dim ensions in regulated string theories. 2, Nucl. Phys. B 275 (1986) 161-184.
  Diseases of triangulated random surface models, and possible cures, Nucl. Phys. B 257 (1985) 433-449.
  J. Ambj m, B. Durhuus, J. Frohlich and P. Orland: The appearance of critical dim ensions in regulated string theories, Nucl. Phys. B 270 (1986) 457-482.
- [63] H.W. Hamber and R.M. Williams: Newtonian potential in quantum Regge gravity, Nucl. Phys. B 435 (1995) 361-398 [hep-th/9406163].

  B.V. de Bakker and J. Smit: Gravitational binding in 4D dynamical trianqualtion, Nucl. Phys. B 484 (1997) 476-494 [hep-lat/9604023].